The Design, Development and Fabrication of a Microwave Proton Ion Source at iThemba LABS

Ceboliyozakha Leonard Ndlangamandla

Thesis presented in fulfilment of the requirements for the degree of Master of Sciences at the University of Zululand

Supervisor: Dr. P. J. Celliers

Accelerator Group

IThemba Labs

Co-supervisor: Prof O. M. Ndwandwe

Dept. of Physics and Engineering

University of Zululand

November 2006

To my parents and my family

DECLARATION

I, the undersigned, hereby declare that the work contained in this thesis is my own original work and that I have not previously in its entirety or in part submitted it at any university for a degree.

Signature: ....

Date: ....

The Design, Development and Fabrication of a Microwave Proton Ion Source at iThemba LABS

Ceboliyozakha Leonard Ndlangamandla

iThemba LABS, P.O.Box 722, Somerset West 7130, Republic of South Africa

November 2006

ABSTRACT

A low-power microwave ion source for the production of protons in the iThemba LABS Van de Graaff accelerator at Faure has been developed. The main advantages of the source are its simple construction, its low power consumption, the small number of parameters that have to be adjusted and the fact that the discharge starts easily. The construction and the operational conditions of the source are discussed. The beam intensities are compared with those of a duoplasmatron ion source in use at iThemba LABS.

ACKNOWLEDGEMENTS

I would like to express my gratitude to my supervisor Dr P. J. Celliers for taking his time and being responsible for me and my study. I wish that my God may bless you now and for ever.

I would also like to express my gratitude to Dr J. J. Kritzinger who built the prototype of the microwave ion source and made it available for studying, for helping me in all the experimental work, and his good guidance. I learned enormously from his knowledge of RF systems, excellent ideas to solve problems in a practical way using simple material, electrical connections and mechanisms. Thank you for your guidance and patience. I also want to thank Dr A. H. Botha for helping me in preparing the poster for the physics conference and also I would like to thank Dr R Thomae for helping me in the simulation of the extraction system of the source and for his excellent suggestions and reviewing of the thesis. I would like to pass my thanks to all the staff of iThemba LABS and especially Dr J. L. Conradie, the Group Head, for being so kind to me during my stay with the group.

I would like to express my gratitude to Mr Hans Delsink for helping me with all drawings and magnet induction. I would also like to express my gratitude and my thanks to all members of the workshop, especially to Lawrence Ashworth for the fast machining of all parts needed to perform the experiments.

I would like to express my gratitude to my university co-supervisor, Prof O. M. Ndwandwe, for opening the opportunity for me to study at higher level. I am grateful to NRF for sponsoring me at the early stage toward my honours degree and thanks to

PBMR for sponsoring me during the work for my masters study. I sincerely appreciate the effort of Prof Charles Dlamini, the former Rector of University of Zululand, for opening study opportunities for needy students like myself, ngithi nje mfoka Dlamini inkosi ikugcine njalo ukwanda kwaliwa nguMthakathi.

Ngithanda ukwendlulisa amazwi okubonga emndenini wami wonke, ngokungigqugquzela kwabo ngokubaluleka kwemfundo ngithi ukwanda kwaliwa nguMthakathi. Ngithi kuwe Mama no Baba uMvelinqangi nezinyanya zakithi nama dlozi akithi abe nani, ngolwasemzini: I like to say thanks for supporting me both financially and also spiritually. Your support opened new opportunities in my life that I will remember life long.

Ngithanda ukwendlulisa amazwi okubonga kuBangani (my brother) naku Zanele Ntshakala (my wife) ngokuba nami ngize ngiphumelele ngibe lapha engikhona namhlanje ngithi sengathi iNkosi inganiphakamisela endaweni ephakeme emndenini nasemphakathini.

I like to thank my friends for their kindness to me and for their loyalty during the course of my study. Ngiyalibonga igalelo lenu, inkosi ibe nani.

TABLE OF CONTENTS

LIST OF FIGURES

LIST OF TABLES

CHAPTER 1

INTRODUCTION AND MOTIVATION

1.1 Accelerators and ion sources

Ion sources some of which are indispensable parts of accelerator systems, because they have to produce those particles which are subsequently accelerated. Ions produced in sources are accelerated to energies that range from a few keV up to a few TeV for numerous applications in medical, physical, biological, pharmaceutical, material science etc. There are various types of ion sources of which some are described in chapter 3.

The need to improve ion sources is illustrated by the numerous testing facilities at accelerator institutions. The task is to optimize beam intensity, the desired ion yield and beam quality of ion sources by using new techniques, processes and materials. International conferences are annually held to discuss the progress in ion source technology.

The importance of testing and developing ion sources at iThemba LABS was soon realized. For this purpose a test stand was built on which various sources were already tested, including sources from other laboratories and companies in South Africa. To view the proposed microwave ion source described in this thesis in context with the bigger picture of this facility, a summary of ion sources and beams produced will be given.

1.2 Background about iThemba LABS

iThemba Laboratory for Accelerator Based Sciences (iThemba LABS) **[Nac76, 89, 90, Con92]**, is a multidisciplinary research centre which provides beams of accelerated charged particles and facilities for particle radiotherapy, basic and applied nuclear and bio-physics research and the production of radioisotopes for nuclear medicine and industry.

Beams of protons, accelerated to 200 MeV and 66 MeV are, respectively, used for proton and neutron therapy. Beams of light and heavy ions, as well as polarized protons, with variable energies are provided for nuclear physics experiments. Beams of light and heavy ions are used for material science.

The laboratory, which became operational during 1986, operates a 200 MeV separate sector cyclotron (SSC) and two solid-pole injector cyclotrons, SPC1 and SPC2. Both have a k-value (for the definition of the k-value see appendix) of 8, and are used for pre-acceleration of light and heavy ions to be injected into the SSC. The staff of iThemba LABS designed and built the machines and beam lines themselves **[Con92, Nac76]**.

SPC1 has an internal PIG ion source, capable of delivering intense beams of light ions and is mainly used for the acceleration of proton beams for proton and neutron-therapy as well as for the production of radioisotopes. Light and heavy ion beams produced in an external electron cyclotron resonance (ECR) ion source and an ion source for polarized protons from a second external ion source are axially injected into SPC2 with a spiral inflector and accelerated before injection into the SSC. The beam energies can be varied over a wide range.

A commercially acquired 6 MV CN van de Graaff accelerator, capable of delivering beams of light and heavy ions with a low energy spread, for a variety of applications is also in operation at iThemba LABS. For the acceleration of various ion species in the Van de Graaff accelerator a duoplasmatron and a PIG ion sources are used.

The control and maintenance of the ion sources in the Van de Graaff differs considerably from those of the cyclotrons. The control of the power supplies and gas flow has to be done over a distance of 5 m inside a high pressured tank of nitrogen gas. Any maintenance involves the ventilation of the accelerator and leak testing of the source before re-installment. This whole process takes hours. In the selection of a new source the severe restrictions in terms of space, high pressure and available power in the Van de Graaff terminal has to be taken into account.

The energy, quality and intensity of the beams delivered by accelerators depend to a large extent on the charge state and intensity that can be obtained from the ion source.

The development and improvement of ion sources are therefore an important part of the activities of any accelerator laboratory.

An ion source that is especially used for the production of high intensity singly charged ions, which is compact and has low power consumption, is the microwave ion source. This kind of source is mainly used in commercial implanters systems and delivers beams free from metallic contamination **[Bro04]**. To evaluate and gain experience with microwave ion sources it was decided to use an existing prototype which has been developed by Dr J. J. Kritzinger and measure its characteristics on the available ion source test bench.

1.3 Motivation for the study

Ion sources are very important devices for the generation of ion beams for various applications. The type of ion sources used at iThemba LABS are the PIG (penning ionization gauge), ECR (electron cyclotron resonance), duoplasmatron source and source for polarized protons (SPI). They have unique designs and use special resources to produce ion beams for their chosen applications. For their correct functioning they are installed either internally inside SPC1 and the Van de Graaff or are used externally (the ECR and SPI).

The proposed Microwave Proton Ion Source (MPIS) differs from these sources in the way the plasma is created. All of them use hot or cold cathodes to excite the plasma except the ECR source that uses Radio Frequency (RF) microwaves. The difference between the MPIS and ECR sources is that the ECRs uses the principle of electron cyclotron resonance to energise electrons and to confine the plasma by using strong radial and axial magnetic fields while the microwave ion source works at an off ECR-resonance.

The microwave ion source has unique operational characteristics. It has no filament and is easy to use. The aim of this work is to understand, develop and improve the source performance with the purpose to obtain characteristics that can favourably compare with the two sources currently in use at the Van De Graaff accelerator.

The main advantages of MPIS sources are:

- It has no filament
- The power consumption is low
- The discharge starts easily
- The construction is simple
- Only a small number of parameters have to be adjusted.
- It can run with reactive gases.
- It can provide low emittance beams.
- *It is free of metallic ion contamination*

Its disadvantage is:

- When using a microwave window with an RF guide the window's lifetime could be limited because of the electron bombardment and metal vapour deposition on the window **[Wol95b], [Bro89a]**.

1.4 Outline of the thesis

- The accelerator facilities are shortly described in chapter 2.
- The ion sources for the accelerators are presented in chapter 3.
- The design and the characteristics of the microwave ion source is presented in chapter 4
- The experimental setup and experimental work are represented in chapter 5.
- The results and their discussion are given in chapter 6.
- The summary and conclusions are presented in chapter 7.

CHAPTER 2

THE ACCELERATOR FACILITIES AT ITHEMBA LABS

2.1 Introduction

The accelerators at iThemba LABS are as follows:

- The Van de Graaff accelerator.
- Separated-sector cyclotron.
- Light-ion injector cyclotron (SPC1).
- Injector cyclotron for both heavy and polarized ions (SPC2).

All these are briefly discussed below accordingly.

2.2 The Cyclotron facilities at iThemba LABS

The final acceleration of charged particles takes place at the SSC after the pre-acceleration of both light and heavy ions by SPC1 and SPC2, respectively. SPC1 has a k-value of 8 and accelerates protons to a maximum energy of 8 MeV. SPC2 and the SSC have k-values (see appendix for explanation) of 10 and 200, respectively.

The RF frequency ranges for all the cyclotrons are from 8 MHz to 26 MHz. Harmonic number 2 and 6 for both SPC1and SPC2 and 4 and 12 for the SSC are used. Both injectors have two 90^0 dees and the SSC two 56^0 dees. After the final acceleration at the SSC, the beam of charged particles is transported through the stainless steel beam pipes, directed and focused by means of dipole and quadrupole magnets to different vaults for nuclear physics experiments **[Con92, Mai02, Nac76, and Mok02]** and radioisotope production.

2.3 Van de Graaff facilities at iThemba LABS

Beam from the Van de Graaff accelerator is mainly used for solid state and material research. It uses a duoplasmatron and penning ion source, which provide both light and heavy ions beams. Figure 2.1 show a layout of the Van de Graaff accelerator and its beamline.

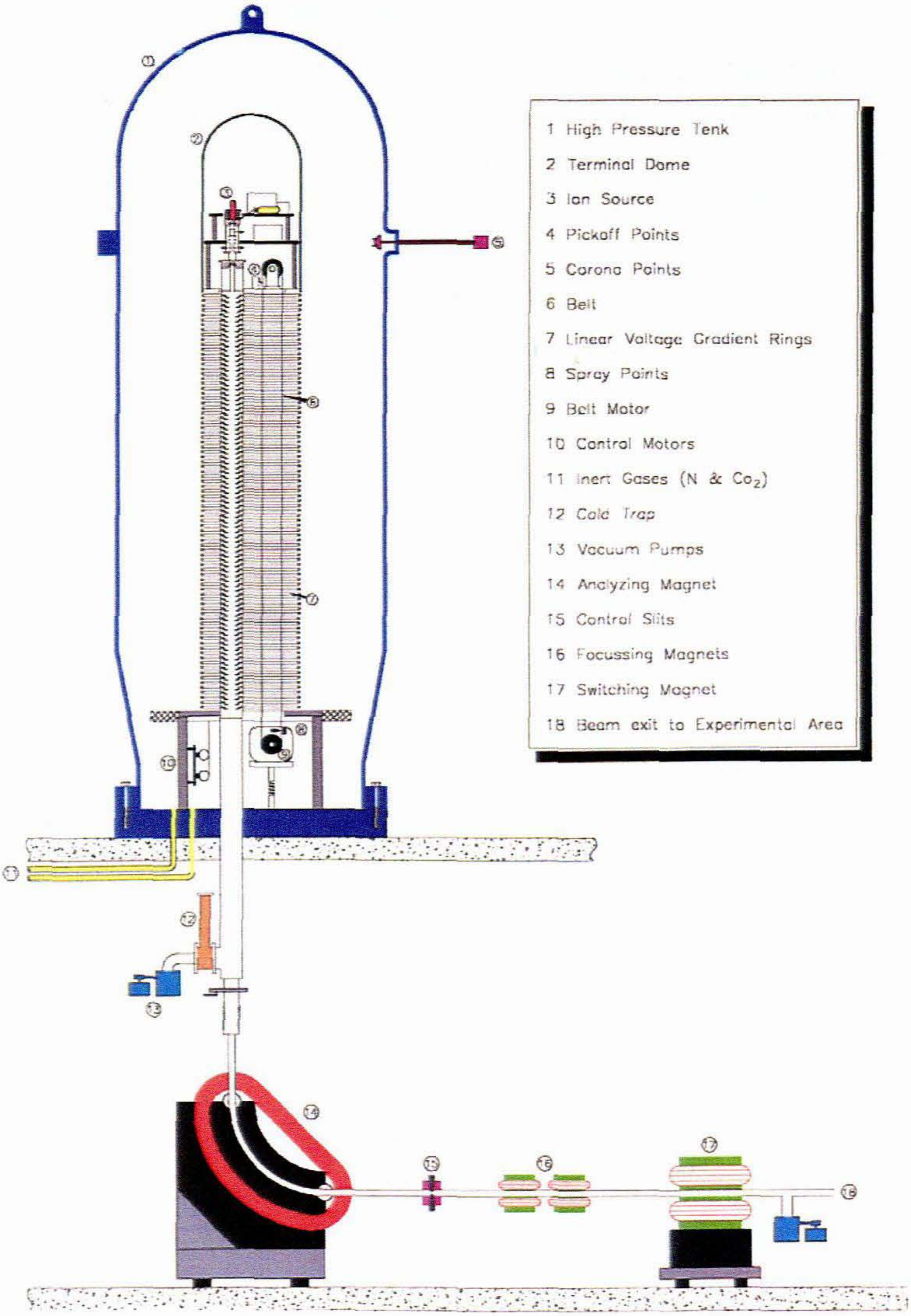

Figure 2.1: The layout of the Van de Graaff accelerator and part of its beam lines at iThemba LABS.

2.4 The separated-sector cyclotron (SSC)

The separated-sector cyclotron accelerates proton beams to a maximum energy of 200 MeV. The SSC has four separated magnet sectors with mass of about 350 tons each and with a sector angle of 34^0. The maximum magnetic field in each sector is 1.256 T **[Con92, Mai02, and Nac76]**. These sectors guide the beam to pass through them up to 350 times at the RF-frequency range of 8 MHz to 26 MHz, using a maximum accelerating voltage of 220 kV **[Mok02]**. The SSC is able to accelerate beams of both light and heavy ions up to Xenon and beams of polarized protons. It also extracts proton beam intensities of 200 μA at an energy of 66 MeV for radioisotopes production. Figure 2.2 shows a cross-sectional diagram of the SSC.

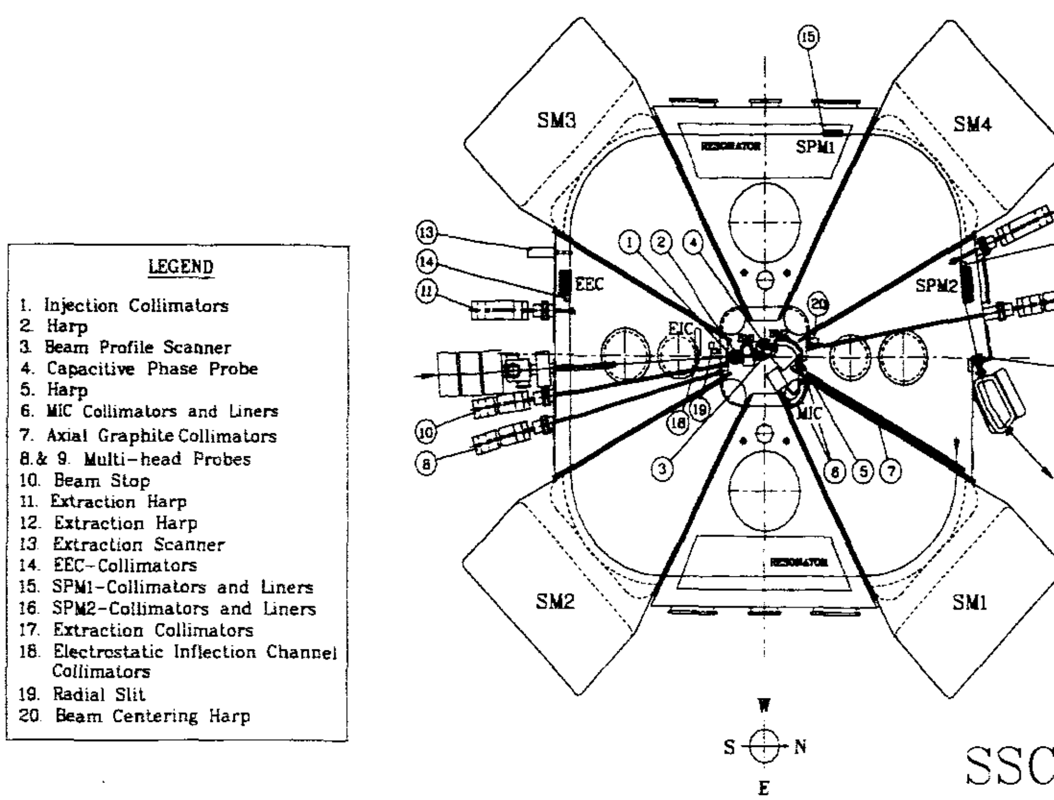

Figure 2.2: A cross-sectional drawing of the separate sector cyclotron at iThemba LABS.

2.5 The light ion injector cyclotron (SPC1)

SPC1, the layout of which is shown in figure 2.3, has an H-type solid pole magnet with four 45^0 radial sectors for vertical focusing, attached to each of the poles. The acceleration system consists of two $\lambda/4$ resonators with two dees each coupled to a 25 kW power amplifier. It accelerates light ions and protons to an energy of 8 MeV for protons. The beam from SPC1 is then injected into the SSC for the final acceleration to an energy of 200 MeV.

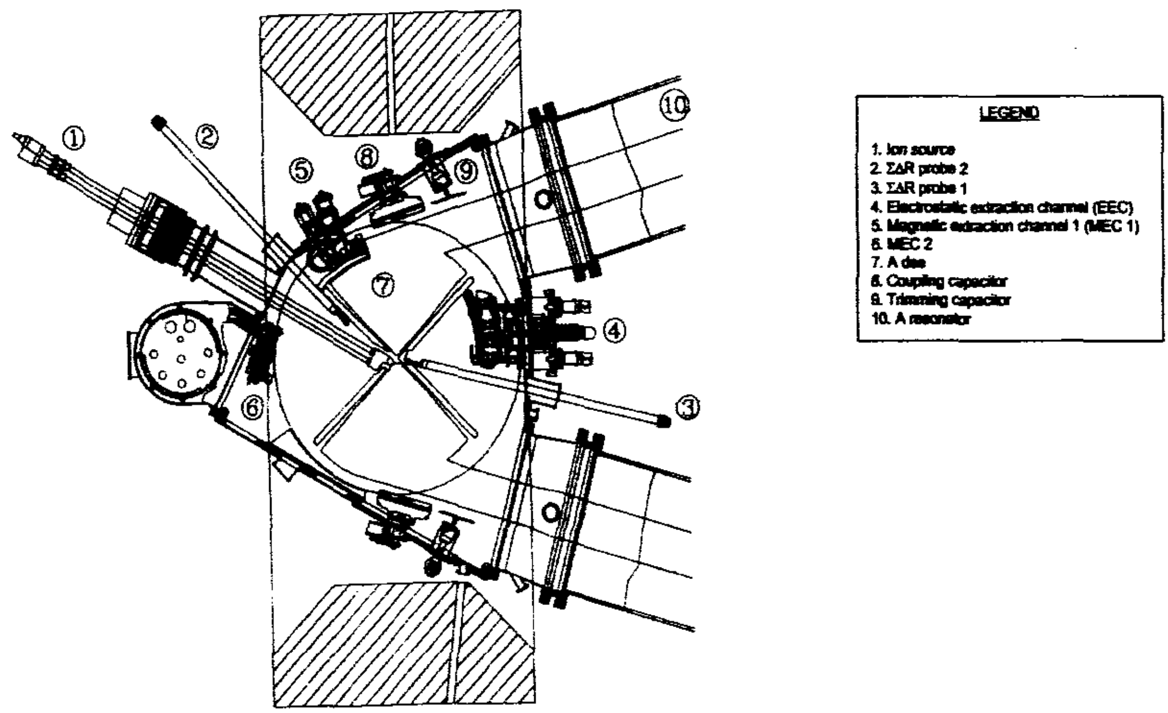

Figure 2.3: A cross-sectional drawing of the SPC1.

2.6 The injector cyclotron for both heavy and polarized ions (SPC2)

The external construction of the SPC2 and SPC1 injectors are similar. In contrast with SPC1, SPC2 (figure 2.4) has an inflector to inject beams from the two external ion sources, the ECR and SPI. SPC2 accelerates beams ranging from light ions e.g. Helium, to heavy ions up to Xe ion. It's k-value is 10. The layout of all the cyclotrons, beamlines and vaults are shown in figure 2.5.

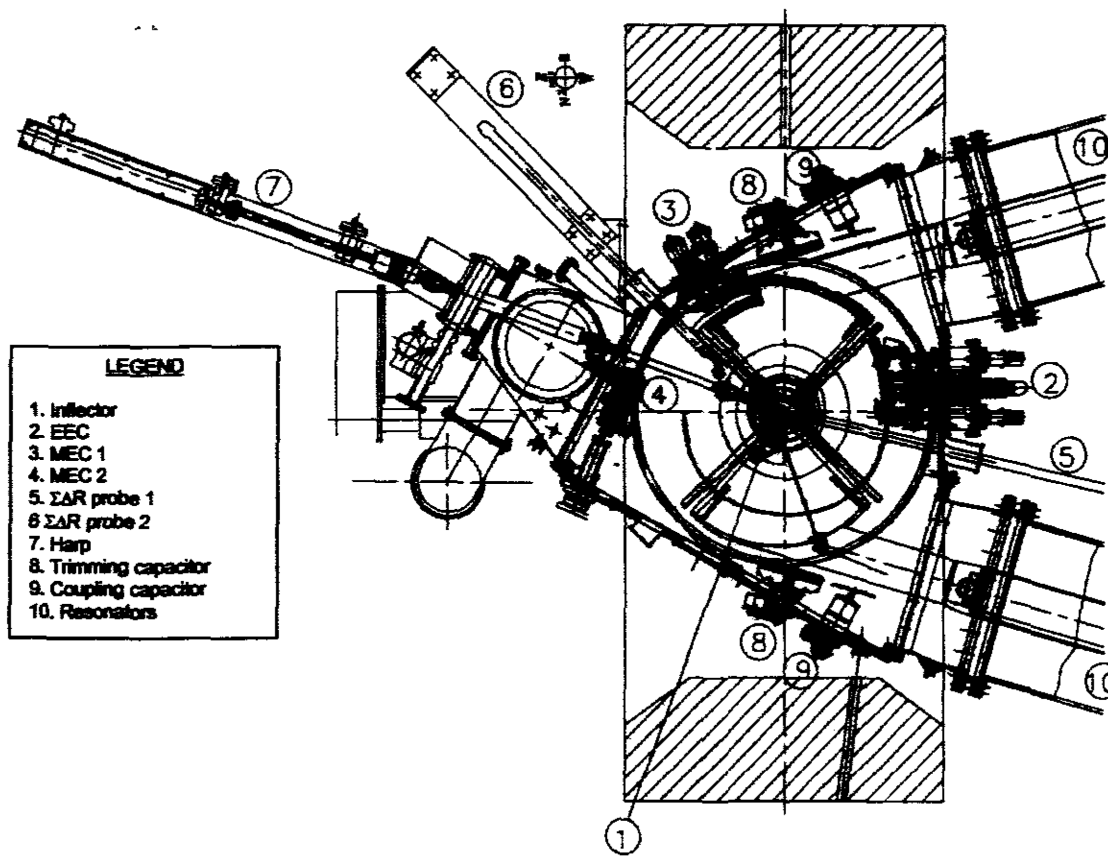

Figure 2.4: A cross-sectional drawing of the SPC2.

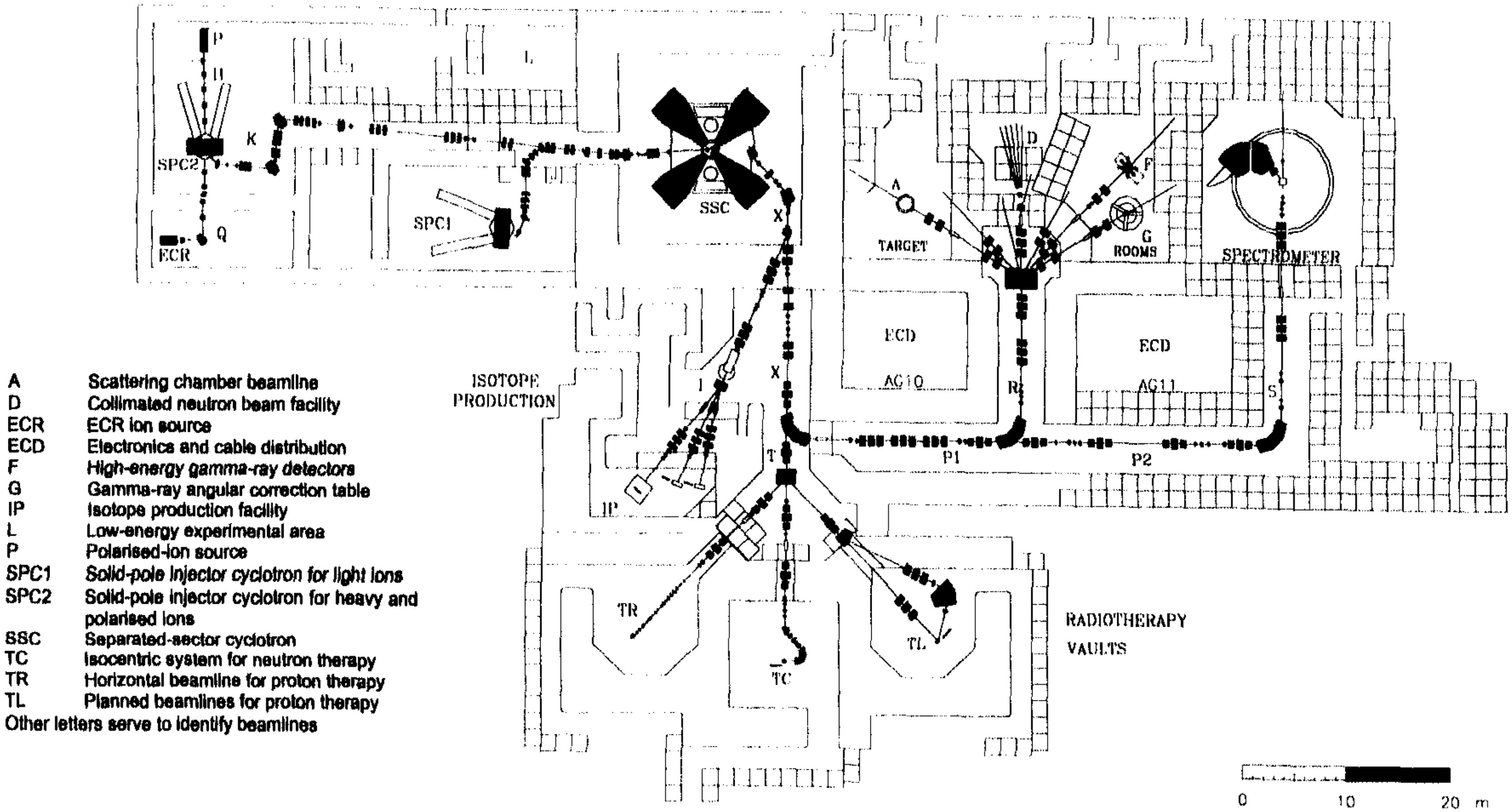

Figure 2.5: The layout of the cyclotron facilities at iThemba LABS.

CHAPTER 3

ION SOURCES

3.1 Ion sources for accelerators

Ion sources used for the acceleration of charged particles are chosen according to their output beams, emittance, ion species, intensity and energy spread. The following ion sources are currently used in many accelerator laboratories

- ❖ PIG ion source.
- ❖ ECR ion source.
- ❖ Multi-cusp ion source.
- ❖ Duoplasmatron ion source.
- ❖ Microwave ion source.

3.2 The PIG ion source

The PIG ion source (invented in 1931) was built to produce light ions in cyclotrons. It uses a cathode, which can be cold or hot (filament), to produce electrons in the discharge chamber for the plasma formation **[Mok02]**. A strong magnetic field confines the plasma inside the plasma chamber in a transverse direction to prevent the electrons from moving sideways as they move repeatedly between the cathode and anti-cathodes iteratively causing ionization through collisions with the gas molecules and atoms **[Bro89c]**.

The PIG ion source consists of a hollow anode cylinder with two cathodes on each end. The ions are extracted sideways through a slit in the anode as is shown in figure 3.1. Sources that operate with the cold cathode are more difficult to start and therefore higher voltages are required. This type of source produces high-intensity protons and other light ions **[Max31]**.

The arc current and voltage of this source can vary from few milliamps to tens of ampere and few hundreds to several kilovolts, respectively, depending on the cathode and gas pressure. The source has a short lifetime because the filament can not withstand the sputtering of ions that strike the filament **[Hil]**.

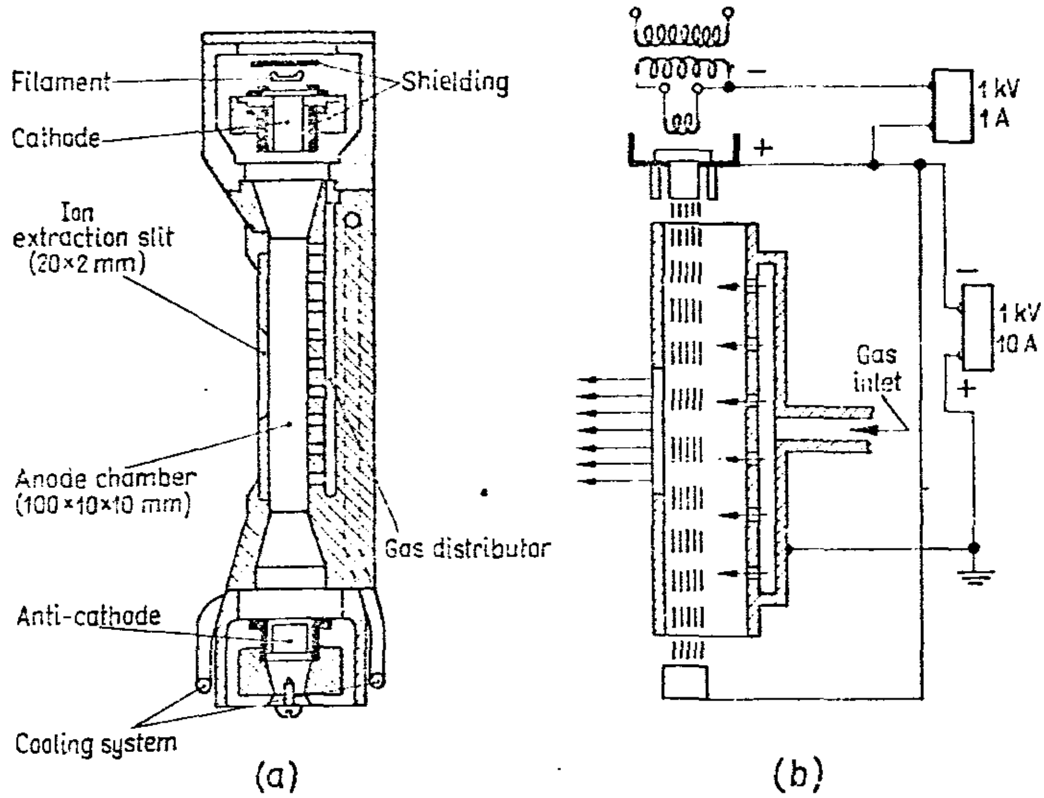

Morozov's high intensity ion source with heated cathode and oscillating electrons: (a) cross sectional view of outlet slit of ion source; (b) block diagram of power supply system for ion source

Figure 3.1: A cross-sectional drawing of the PIG ion source.

3.3 The ECR ion source

The ECR ion source, proposed by R Geller in 1965, produces high currents of ions with high charge states **[Gel69]**. ECR ion sources were designed to overcome the limitations of the PIG ion sources such as for instance the low charge states and the erosion of the slits and cathodes. An ECR ion source uses microwave energy to create the plasma which is then confined by radial and axial magnetic fields. The radial field is formed by permanent hexapole magnets and the axial field by coils.

The axial magnetic field can be adjusted to create an electron-cyclotron-resonance zone within the plasma. This ECR resonance allows continuous acceleration of electrons by the electrical field of the microwave and creates ion beams of high charge states **[Wol95d, Hil]**.

This source has the following characteristics

❖ It has a long lifetime (about a month without maintenance) and operates reliably.

❖ It can ionize any element in the periodic table with low gas consumption.

❖ Beam can be produced by using gasses, liquids, organic metal compounds and metals, i.e. both volatile and non-volatile elements gas can be used.

The figure below shows a cross-sectional drawing of an ECR ion source.

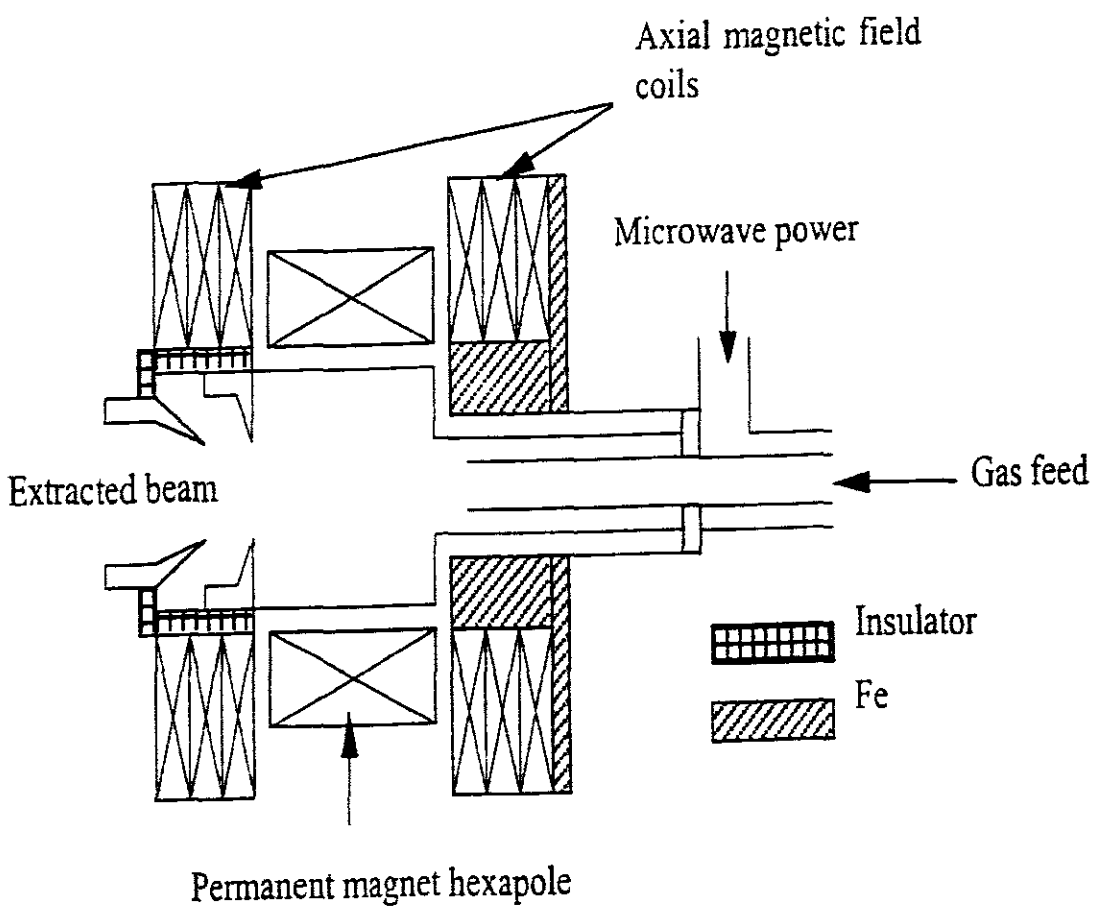

Figure 3.2: A cross-sectional drawing of the ECR ion source [**Mok02**]

This source is capable of delivering ions with very high charge states and allows therefore for higher energies. The maximum energy to which a cyclotron can accelerate an ion is proportional to the square of the charge state of the ion.

3.4 The multi-cusp ion source

The multi-cusp ion source, introduced in 1980 and shown in figure 3.3, is capable of producing high current density and high power beams of energetic particles and is used amongst others for fission research and ion implantation. This source can produce both positive and negative ion beams for accelerators **[Wol95a]**.

The ionizing electrons are produced by a tungsten filament cathode which limits the lifetime of the source **[Mok02]**. In this source the plasma chamber walls form the anode and the confinement of the plasma is done by permanent magnets.

Multi-cusp ion sources are simple and easy to operate. In the construction of the source there are three important parts that play a role in the formation of a plasma.

- The filament acting as a cathode.
- The plasma chamber which forms an anode.
- The outlet electrode or the plasma electrode

This source can either be operated by a filament or an RF antenna or coupling loop. If the source is operated with a RF antenna the RF generator and antenna must be fully matched. The main advantage of the multi-cusp ion source is that it is capable of delivering very high intensity beams of good quality **[Wol95a]**. The plasma is formed by the ionizing electrons produced by the filament which is biased negatively with respect to the anode. The anode is located in the field free region inside the plasma chamber. The plasma density depends on the length of the plasma chamber, magnet geometry and on the discharge current and voltage.

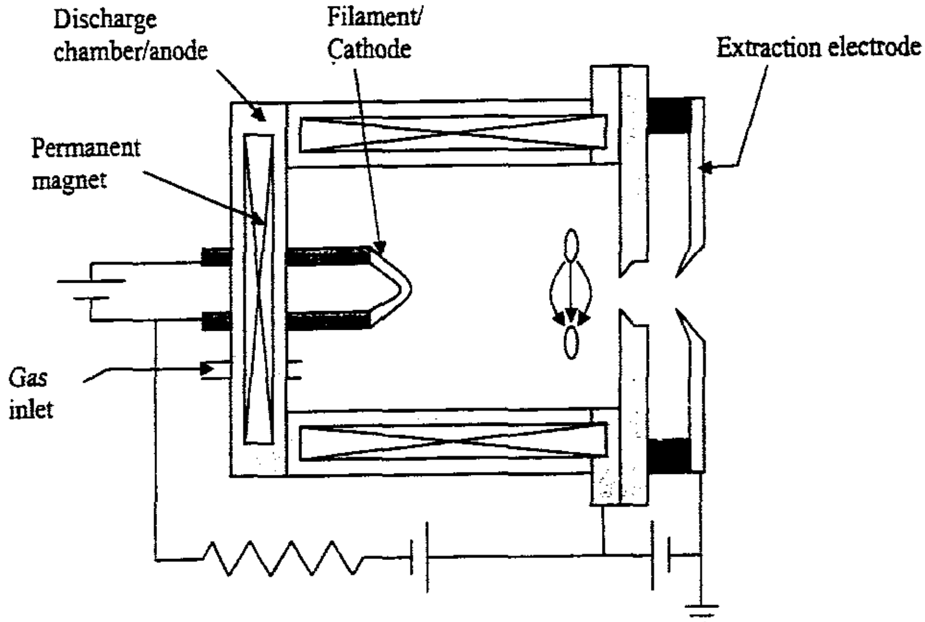

Figure 3.3: A cross-sectional drawing of a multi-cusp ion source **[Wol95a]**

3.5 The duoplasmatron ion source

The duoplasmatron uses a filament, which can be cold or hot that produces the electrons for the plasma. It uses a cooling system and permanents magnets or electromagnets. It has been in use for many years for the production of both high proton current beams and low charged-state, positive heavy ions. Its discharge plasma is confined by the magnetic field. This source uses the anode and intermediate electrode which are made of ferromagnetic material which forms the pole pieces of the magnetic yoke **[Mok02]**.

In the diagram of the source shown in figure 3.4, there are separate regions with different plasma densities. The most dense plasma region with a high degree of ionization exists near the anode. The ions are extracted through a small hole in the anode **[Hil]**. Solenoid magnets around the plasma chamber provide the magnetic field to confine the plasma. The extracted current from the source depends on the plasma density in the extraction region. This source operates at a pressure of 10^{-3} to 10^{-6} mbar. At iThemba LABS this source is capable of producing proton beams up to approximately 34 μA **[Hil, Con92, Eis05, and Mok02]**.

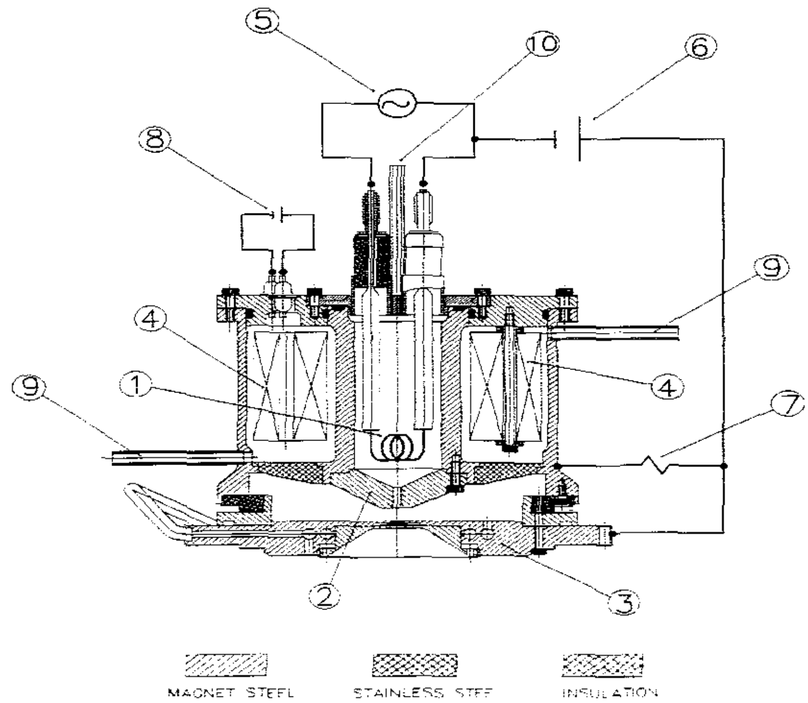

Figure 3.4: Cross-section of a hot-cathode duoplasmatron ion source showing: (1) the cathode, (2) the intermediate-electrode, (3) the anode, (4) the magnet windings, (5) the filament power supply, (6) the cathode power supply, (7) the 2.4 kΩ intermediate-electrode resistor, (8) the magnet power supply, (9) the coolant connections for the magnet windings and (10) the gas inlet. The source has a diameter of 130 mm and a length of 120 mm **[Eis05]**.

3.6 The compact microwave ion source

A microwave ion source, shown in figure 3.5, consists of a RF cavity which is also the plasma chamber (the plasma chamber may be separated by means of isolating material e.g. quartz). The microwave power can enter the cavity by means of an antenna or RF window.

The magnetic field is produced by permanent magnets: CoSm or NdFe. The frequency is usually 2.45 GHz because cheap and reliable RF generators are available. By covering the plasma chamber by boron nitrite, (BN), the wall temperature can be increased which will lead to higher efficiency.

The plasma chamber can be made of Cu, stainless steel, Al or quartz. There is an upper limit on the electron density in a plasma in the absence of a magnetic field **[Wol95b]**, $n_{ep} \leq 1.1*10^{10} f^2 cm^{-3}$ with f in GHz. If the density exceed this value most of the microwave power is reflected back. If however the magnetic field is higher than predicted by the ECR principle the microwave power will be absorbed and the current will increase.

Figure 3.5 shows a compact microwave ion source which is able to produce a beam current of several milliamperes through a 2 mm diameter aperture. It uses permanent magnets to confine the plasma instead of a solenoid. This source is 65 mm height and 50 mm width. This compact microwave ion source works at a frequency of 2.45 GHz and a power consumption of 7- 30 W to create a plasma. At a power of 400 W the source can deliver a current density of 200 mA cm^{-2}. It also provides a low emittance of 10^{-2}mm mrad and a high brightness of 10^{11} Am^{-2}rad^{-2} beam **[Bro04, Bro89e]**.

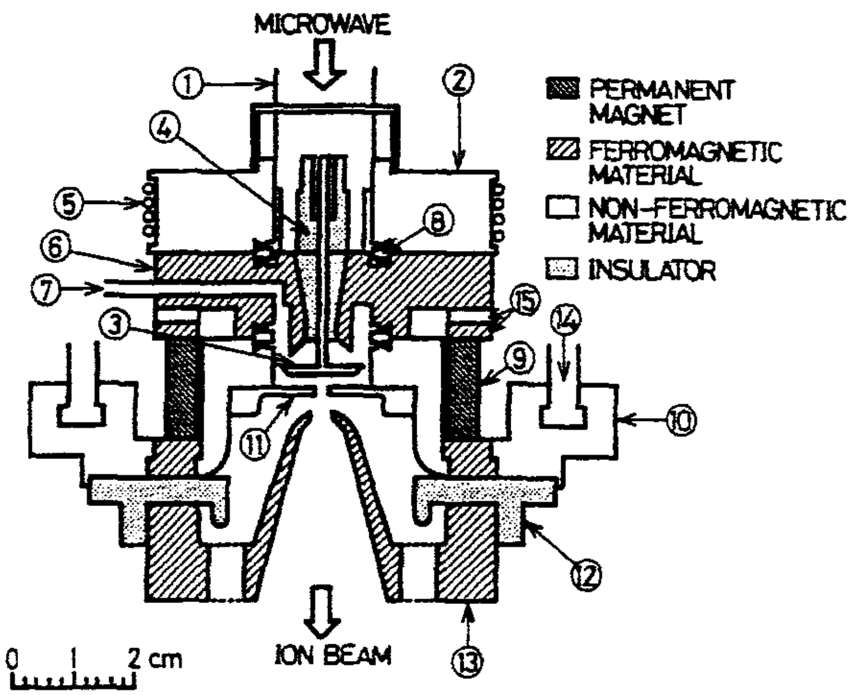

A compact microwave ion source using a permanent magnet: 1, sealed coaxial connector; 2, top flange; 3, antenna; 4, boron nitride; 5, sheath heater; 6, middle flange; 7, gas inlet; 8, copper gasket; 9, permanent magnet; 10, base flange; 11, plate with an extraction aperture; 12, insulator; 13, extraction electrode; 14, coolant; and 15, spacers

Figure 3.5: A cross-sectional drawing of the compact microwave ion source **[Bro04, Bro89e]**

To develop and improve our microwave source at iThemba LABS, some ideas from the above mentioned source were used.

The figure below shows the magnetic flux lines in the extraction system of this source. It is easily seen that the magnetic field lines allow the electrons to spiral around the field lines close to the extraction aperture.

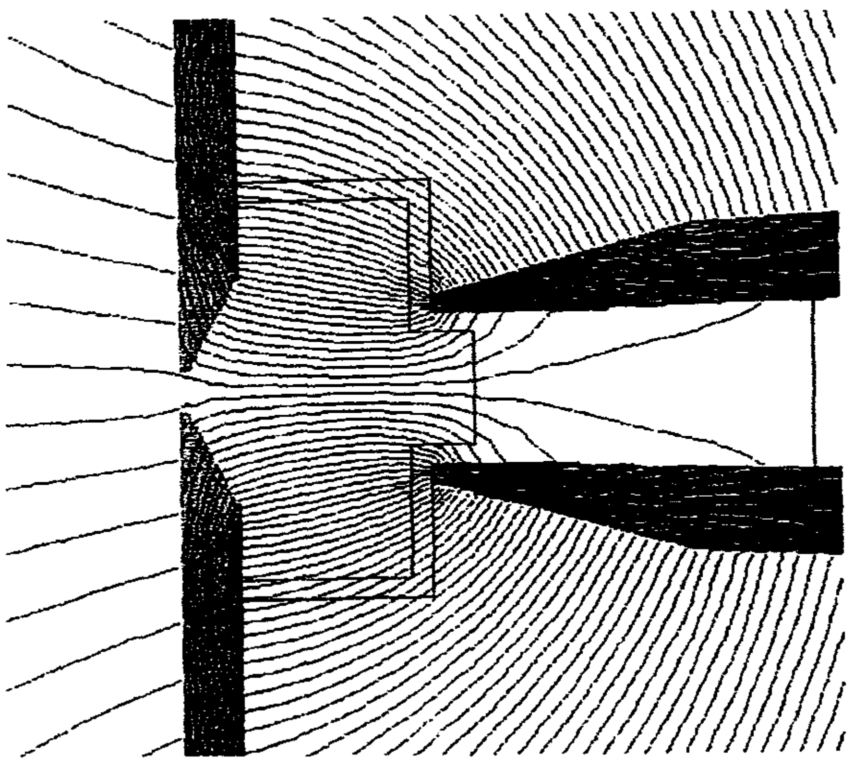

Figure 3.6: Magnetic field lines around the extraction system of the compact microwave ion source **[Bro04]**.

CHAPTER 4

THE DESIGN AND CONSTRUCTION OF THE ITHEMBA LABS MICROWAVE ION SOURCE

4.1 The background of the microwave ion source

Microwave ion sources are classified **[Tay93]** according to two principles: an ion source that operates on the principle of electron cyclotron resonance (ECR) to produce multiple charged ions and an ion source that uses the off-resonance principle to produce higher currents for single charged ions. They use frequencies in the GHz range as is the case with ECR source. The latter will be the focus of this study.

Microwave ion sources for the production of multiple charged ions were developed in 1960s by R. Geller. The ionization was achieved using the ECR principle by heating electrons using microwaves and confining the plasma in a magnetic bottle **[Wol95b]** produced by hexapole magnets and helmholz coils.

Some examples of microwave ion sources to produce high currents of single charged ions using off-resonance ionization are the following: In 1977 Sakudo built a microwave ion source using an antenna to transmit the microwaves into the ion source chamber through a microwave window. He used coils to produce the axial magnetic field to confine the plasma. In 1984 Ishikawa developed a compact microwave ion source using permanent magnets **[Wol95b]**.

For the present study we are using a microwave ion source designed and built by J. J. Kritzinger. It was further improved by using the ideas we developed during the course of the study.

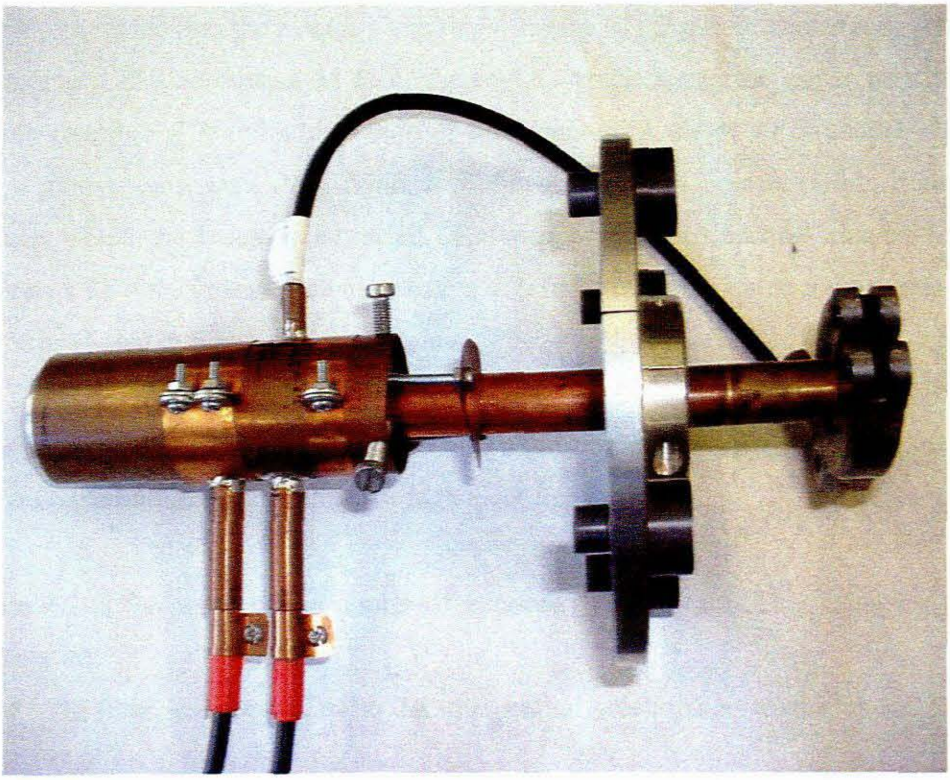

Figure 4.1: The microwave ion source without the magnets and extraction system as designed by J. J. Kritzinger.

4.1.1 The design and the construction of the microwave ion source at iThemba LABS

Photos of the microwave source are depicted in figure 4.1 and 4.2 and a cross-sectional drawing in figure 4.3. Figure 4.2 is a modified version and consists of the following parts. They are the resonator that excites the electrons to ionize the hydrogen atoms in the plasma chamber shown in figure 4.4, the outlet electrode figure 4.5, ground electrode figure 4.6 and the three ferrite magnets, figure 4.7. It has a connection for the co-axial cable from the microwave generator and one for measuring input power.

The source with its inner and outer conductors and short-circuit plate forms a $\lambda/4$ resonator, which makes it possible to start the source. The dimensions of both the inner and the outer conductors are chosen to have a characteristic impedance of nearly 50 Ω. The resonator of the source can be fine tuned by moving the short-circuit plate and the position of the input cable slightly up or down.

The H_2 gas is fed into the plasma chamber by means of a 2 mm diameter copper tube, protruding a PVC or shapal-M disk, figure 4.8, which forms the upper part of the plasma chamber. The cylindrical side of the chamber, made of Al or shapal-M, fits into a groove on a steel disk, figure 4.5, that has a small hole of 1 mm diameter through which the beam is extracted. The two or three cylindrical shaped ferrite magnets with a thickness of 12 mm, figure 4.7, fits around the outer conductor of the source as shown in figure 4.2 or 4.3 below.

The source should operate or run under the condition of a low pressure, low gas and power consumption and operate on a high electrical potential.

Figure 4.2 is the photo of the improved microwave ion source. The following parts can be seen:

- The four isolator pillars to fix the ground steel flange to the upper flange which is at high potential.
- Two ferrite magnets
- Top part of the H_2 gas-inlet into the source

The two vespal (white) isolators are levers for the fine tuning of the position of the short-circuit plate and the microwave coupling point. The fine tuning of the position of the short-circuit plate is done by rotating the lever which is seen as a vertical white strip on the left of the left pillar. This lever turns an off-centred disk that moves a spring up and down and therefore also the short circuit plate that is connected to two bolts on the spring lever. The coarse movement on the short-circuit plate is done by moving the bolts of which one of them is visible on the source.

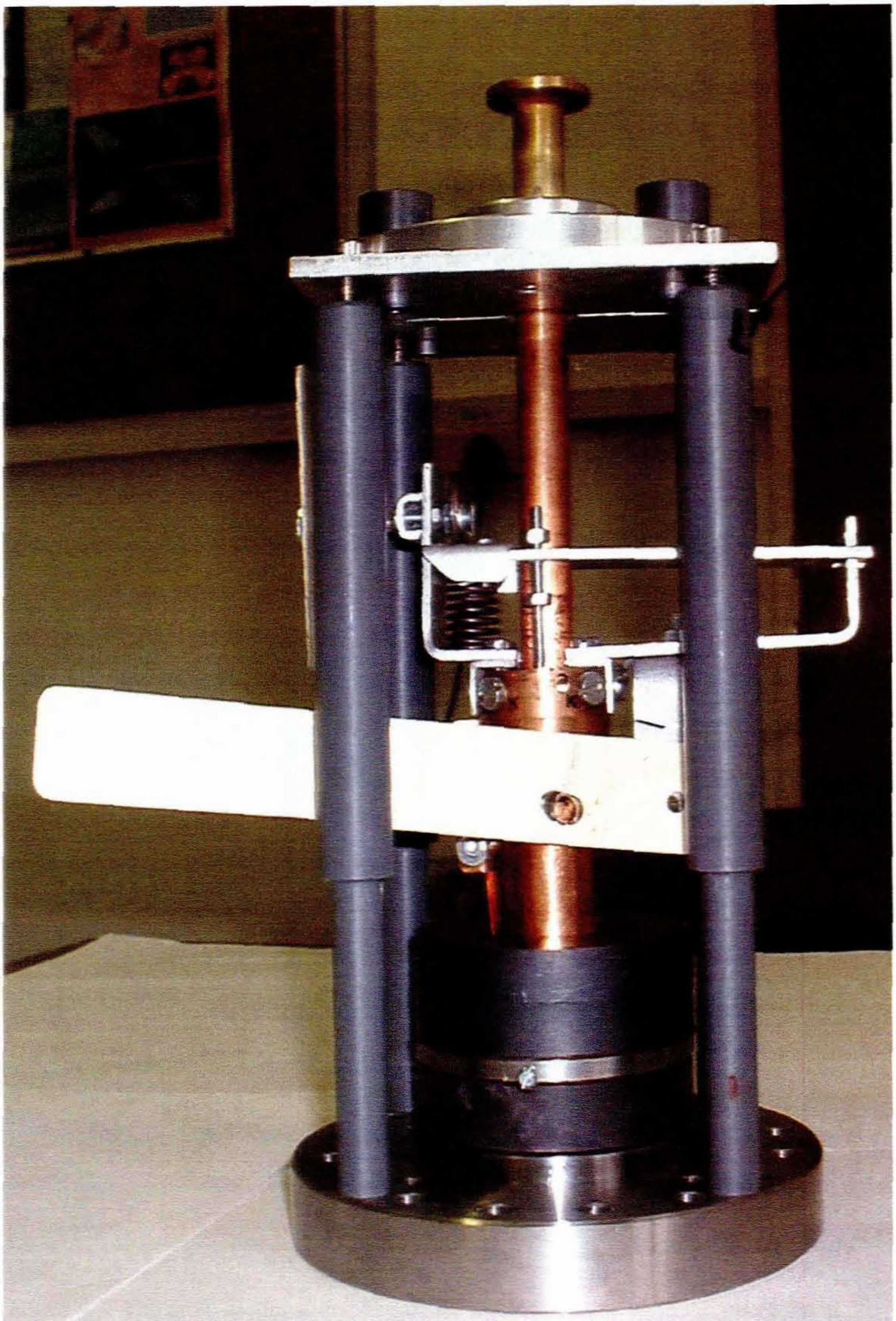

Figure 4.2: A photo of the optimized microwave ion source

Figure 4.3 shows the cross-sectional drawing of a microwave ion source.

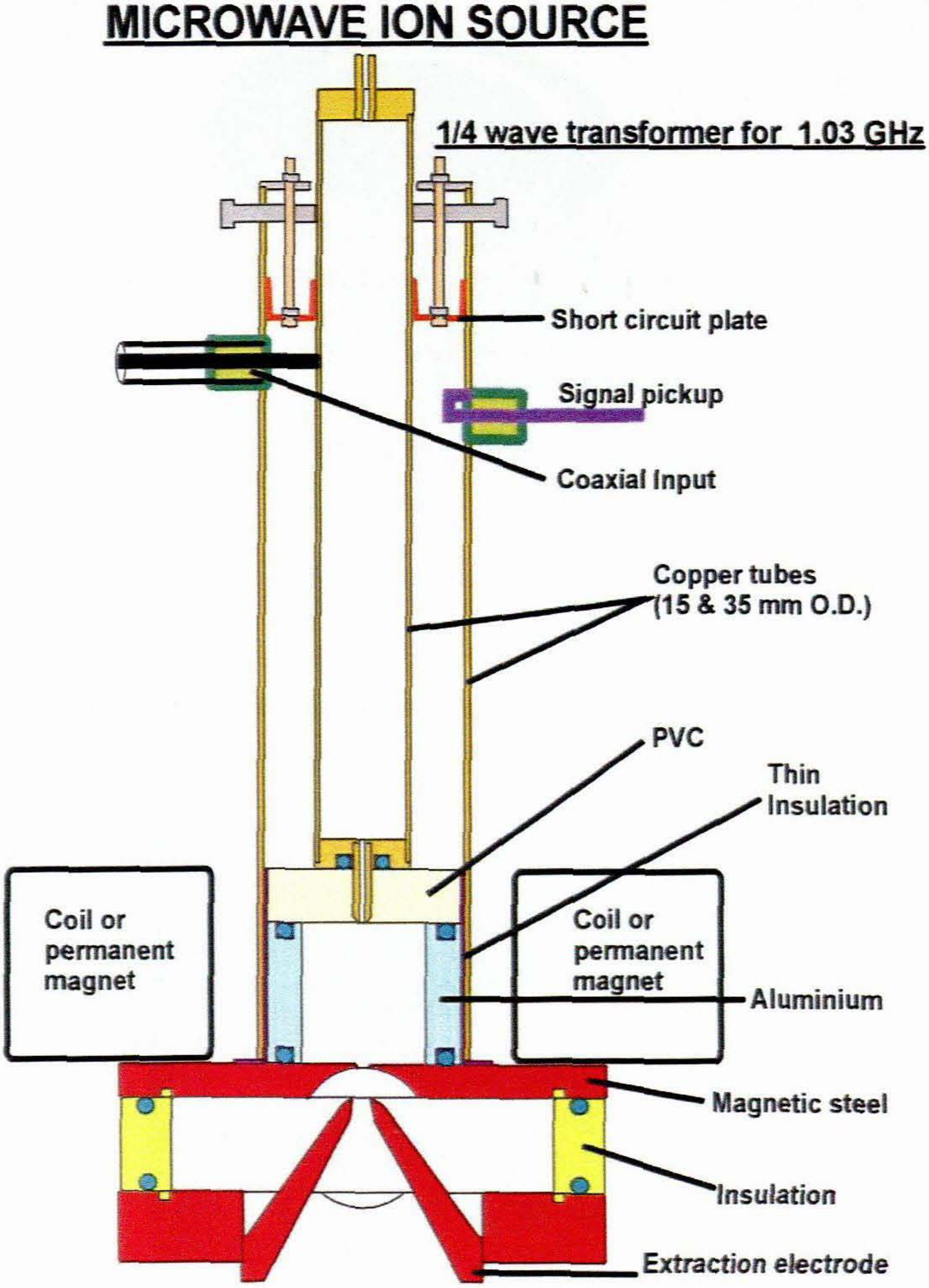

Figure 4.3: The cross-sectional drawing of the microwave ion source in operation at iThemba LABS.

Figure 4.4 shows a picture of the plasma chamber that is used in the source. The plasma chamber was later changed to shapal-M.

Figure 4.4: A photo of the plasma chamber

Figure 4.5 is a picture of the outlet electrode. This part of the source can either be magnetic or non magnetic with an outlet aperture of 1 mm diameter. The design of this part will later be changed to have a conical shape and made of aluminium.

Figure 4.5: A photo of an outlet electrode

Figure 4.6 shows a photo of the ground electrode with an aperture of 4 mm diameter. The ground electrode shown in figure 4.6 is on ground potential.

Figure 4.6: A photo of a ground electrode

Figure 4.7 shows the magnets for the confinement of the plasma in the source. They are 12 mm thick. The outer and the inner diameter are 80 and 40 mm, respectively. The magnetic field of these magnets can be adjusted by induction using *i*Themba LABs induction magnet.

Figure 4.7: A photo of the ferrite magnet

Figure 4.8 is a picture of the PVC disk that forms part of the top of the plasma chamber. This was later replaced by a shapal-M disk.

Figure 4.8: A photo of the PVC disk

The microwave power is fed into the resonator through a RG58 co-axial cable to the ion source. A pick-up signal, generated by a microwave diode inside the resonator, is measured by a voltmeter.

The tuning of the resonator of the microwave ion source to create a quarter standing wave resonance is done by means of the short-circuit plate, figure 4.9. The inner and outer circumference is cut into strips called fingers to make good electrical contact with the inner and outer conductors. These fingers also secure the positions of the inner and outer conductors. Figure 4.9 is the picture of the short-circuiting plate.

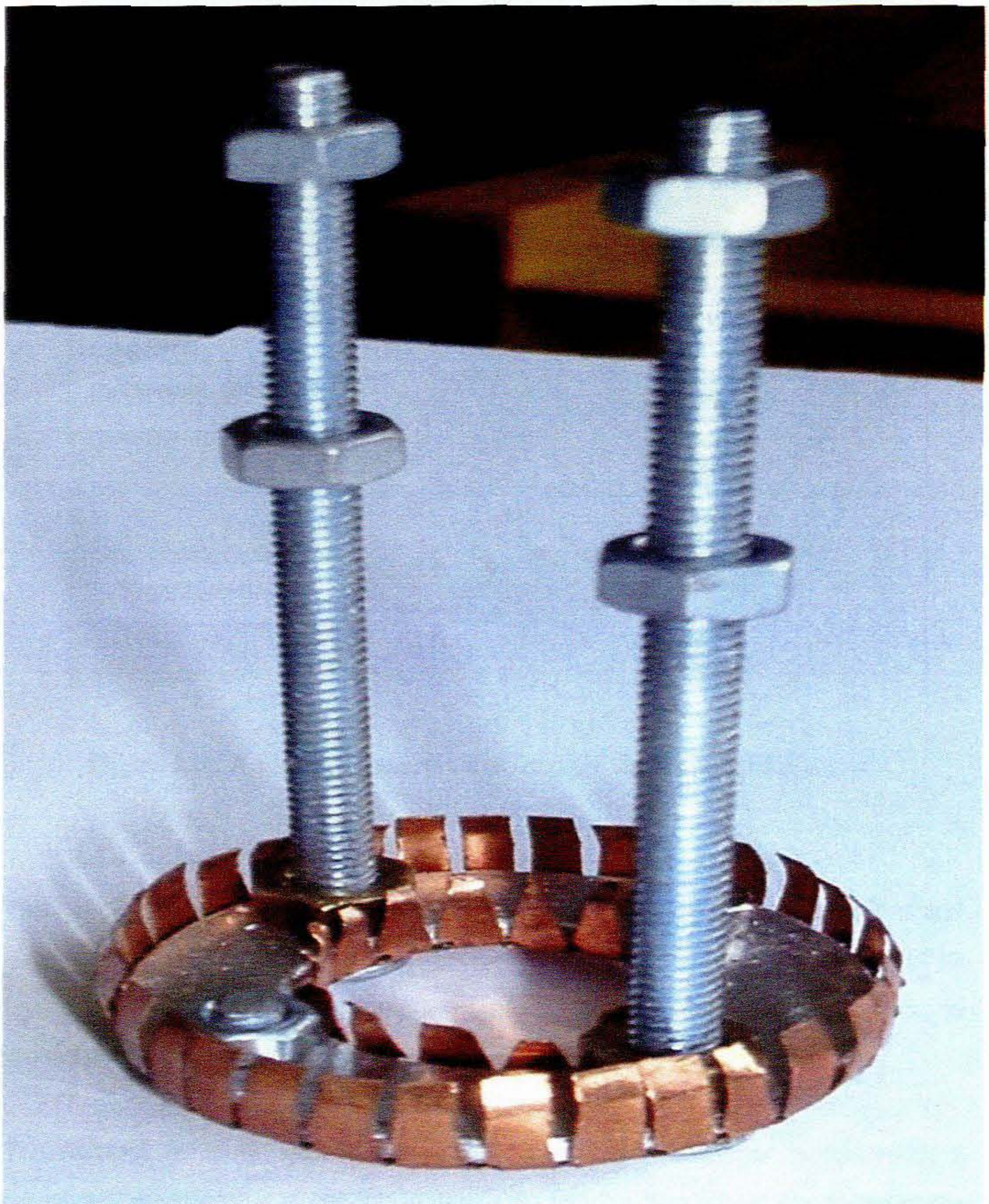

Figure 4.9: A photo of the short-circuiting plate with the fingers

Figure 4.10 shows the electrical connections for the microwave ion source. This includes the 1.265 GHz microwave generator, circulator, dummy load, the trombone line, co-axial lines and multimeters.

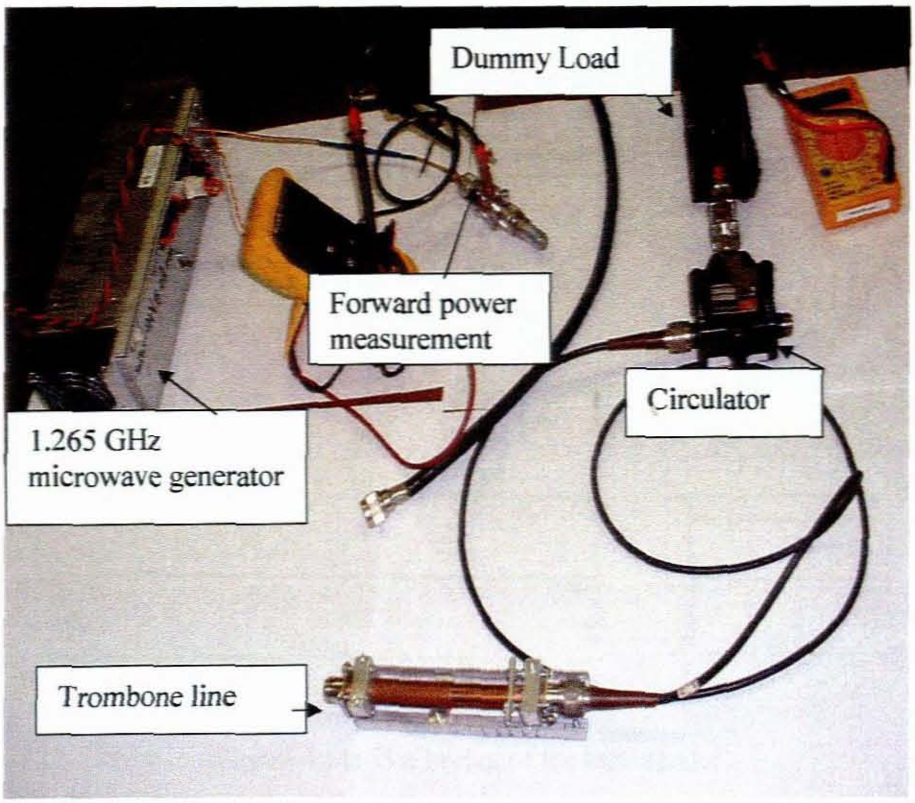

Figure 4.10: A photo of the apparatus used for the testing of the source

4.1.2 The ion source test stand

The source is mounted on a high voltage platform test stand to accelerate the ions and measure its characteristics. Figure 4.11 and 4.12 show a photo and the drawing of its layout. The gas, the vacuum equipment, power supplies and faraday cups are on ground potential.

The vacuum pumping system consisted of two turbo molecular pumps, with a capacity of 60 l/s each and one fore-pump. Two faraday cups are used to measure the beam current, one direct behind the source and the second one at the end of the beam line behind the analyzing magnet.

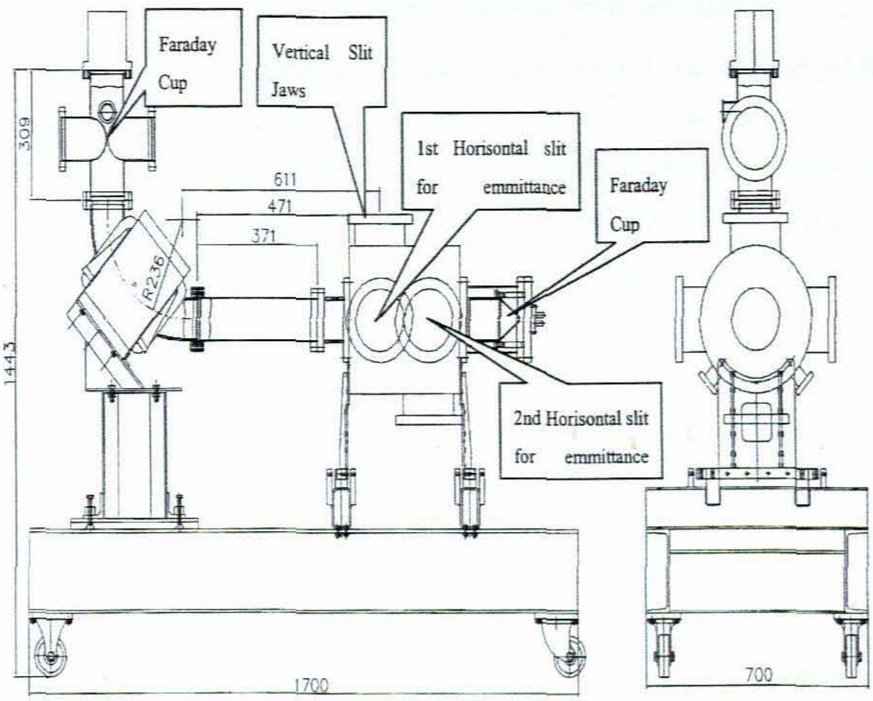

Figure 4.11: The layout of the test stand.

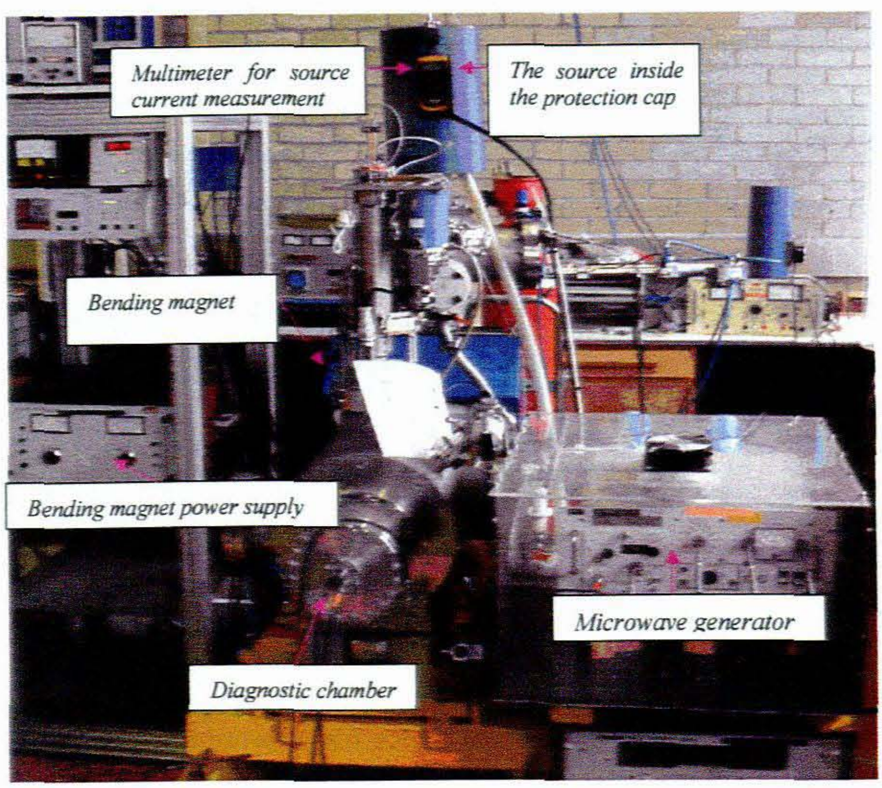

Figure 4.12: The microwave ion source mounted on the test stand

4.1.3 Microwave power coupling and impedance matching

The microwave power generator is coupled to the source by a 50 Ω co-axial cable through a trombone unit shown in figure 4.10. Transferring the power between the microwave generator and the plasma chamber is ensured by constructing the resonator of the ion source with a characteristic impedance of 50 Ω. The reflected power can be measured by measuring the voltage induced on a diode-resistor combination in the circulator.

The length of the co-axial line may have unwanted standing waves that cause resonance at other frequencies. The position of these unwanted standing waves can be changed by tuning the trombone line to obtain minimum reflected power. Both the microwave power coupling point and the short-circuiting plate are movable (up or down) for matching of the microwave generator and the ion source resonator. Resonance is found by moving the short-circuit plate slowly up and down until the reflected power is measured to be at minimum on the meter on the circulator.

The importance of the position of the coupling point on the resonator was investigated by calculating the impedance of the resonator as a function of the entry point.
The input impedance of the transmission line is given by the equation **[Tra63]**:

$$Z_i = Z_0 \frac{Z_R + Z_0 \tanh \gamma d}{Z_0 + Z_R \tanh \gamma d} \qquad (4.1)$$

with Z_0 the characteristic impedance of the line and Z_R the receiving end impedance and d the line length. The phase is given by:

$$\gamma = \alpha + j\beta \qquad (4.2)$$

where α is the real part of the resistance and β is the imaginary part.

The impedance at the coupling point is the impedance of the segment of the line from this point to the short-circuit plate in parallel with the impedance of the remaining section of the line as seen from the coupling point. The first impedance is called Z_l and that of the remaining section Z_r. For the left-hand side the relation, $Z_l = 0$, identifies the short-circuit part and the right-hand side identifies Z_r as ∞.

4.1.3 Microwave power coupling and impedance matching

The microwave power generator is coupled to the source by a 50 Ω co-axial cable through a trombone unit shown in figure 4.10. Transferring the power between the microwave generator and the plasma chamber is ensured by constructing the resonator of the ion source with a characteristic impedance of 50 Ω. The reflected power can be measured by measuring the voltage induced on a diode-resistor combination in the circulator.

The length of the co-axial line may have unwanted standing waves that cause resonance at other frequencies. The position of these unwanted standing waves can be changed by tuning the trombone line to obtain minimum reflected power. Both the microwave power coupling point and the short-circuiting plate are movable (up or down) for matching of the microwave generator and the ion source resonator. Resonance is found by moving the short-circuit plate slowly up and down until the reflected power is measured to be at minimum on the meter on the circulator.

The importance of the position of the coupling point on the resonator was investigated by calculating the impedance of the resonator as a function of the entry point.
The input impedance of the transmission line is given by the equation **[Tra63]**:

$$Z_i = Z_0 \frac{Z_R + Z_0 \tanh \gamma d}{Z_0 + Z_R \tanh \gamma d} \tag{4.1}$$

with Z_0 the characteristic impedance of the line and Z_R the receiving end impedance and d the line length. The phase is given by:

$$\gamma = \alpha + j\beta \tag{4.2}$$

where α is the real part of the resistance and β is the imaginary part.

The impedance at the coupling point is the impedance of the segment of the line from this point to the short-circuit plate in parallel with the impedance of the remaining section of the line as seen from the coupling point. The first impedance is called Z_l and that of the remaining section Z_r. For the left-hand side the relation, $Z_l = 0$, identifies the short-circuit part and the right-hand side identifies Z_r as ∞.

Table 4.1: The characteristic data of the microwave ion source calculated for a resonance frequency of f = 1.03 GHz:

f =	1.03E+09	Hz	operating frequency
a =	7.50E-03	M	outer radius of inner tube
b =	1.70E-02	M	inner radius of outer tube
R =	2.56E-01	Ω/m	= 2.61e-7*f^0.5*(1/2/p/a+1/2/p/b)
Pi =	π		
L =	1.64E-07	H/m	= 2e-7*ln(b/a)
C =	6.78E-11	F/m	= 5.55e-11/ln(b/a)
Z_0 =	4.91E+01	Ω	= (L/C)^0.5
α =	2.61E-03	neper/m	= R/2/Z0
ß =	2.16E+01	radiale/m	= 2*p*f/c

R, L and C are the resistance, the inductance and the capacitance per meter of the conductor, respectively.

If $Z_l = 0$ and $Z_r = \infty$ the input impedance is given by:

$$Z_i = Z_0 \tanh j\gamma d \tag{4.3}$$

and $$Z_i = \frac{Z_0}{\tan(\gamma d)} \tag{4.4}$$

The characteristics impedance **[Tra63]** given as:

$$Z_0 = \sqrt{\frac{R + jL\omega}{G + jC\omega}} \tag{4.5}$$

The parallel impedance of the combination was calculated using the complex facility of the windows program excel.

Figure 4.13 shows the graph of the impedance as a function of the length of the inner conductor at a frequency of 1.03 GHz. The resonance has been obtained for the resonator length of 73.4 mm. The coupling point is approximately 1 mm away from the short-circuit plate. These results show the position of the entry or couple point is very critical and should be taken in consideration when studying the source.

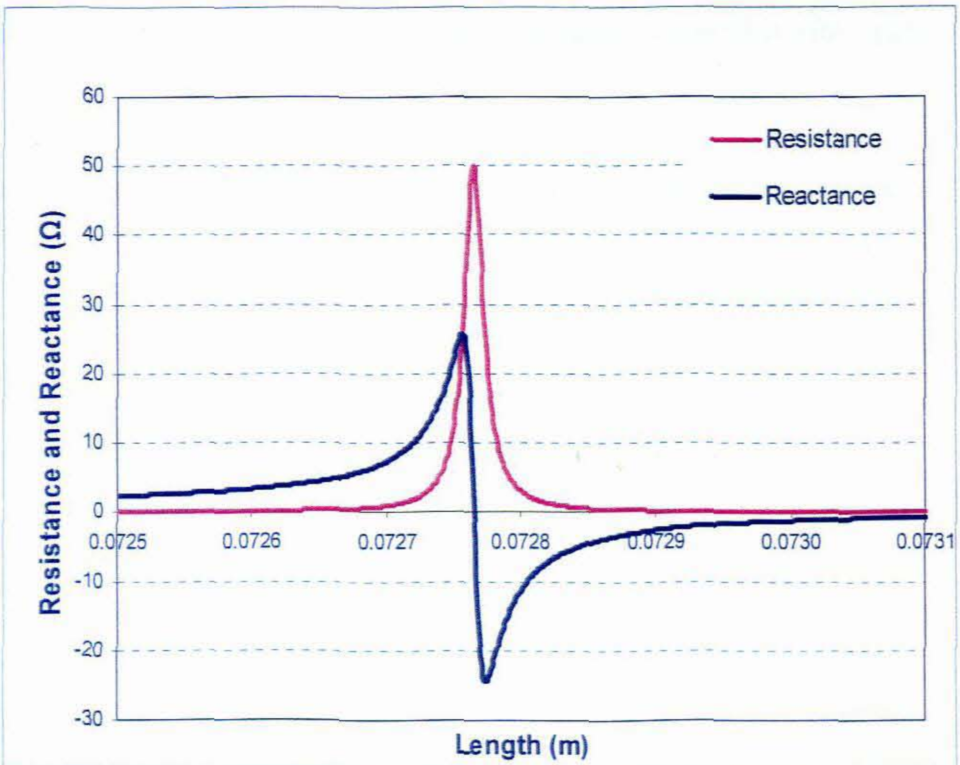

Figure 4.13: Calculated resistance and reactance at the coupling point as a function of the resonator length.

4.1.4 Resonance

The resonator can be described as a co-axial line consisting of a pair of concentric conducting copper cylinders. It has a total resistance per unit length R_i including both conductors as well as capacitance C and the inductance L per unit length.

The resonator can be presented by a diagram shown in the figure below.

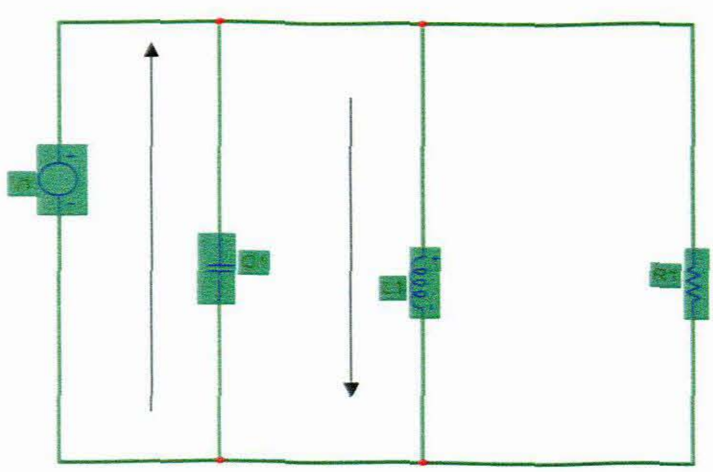

Figure 4.14: The circuit diagram of the resonator

At resonance the voltage across inductance and capacitance is equal but with a phase difference of 180^0.

The plasma can be considered to be a resistive dielectric **[Bro04]**.When the source is switched on the impedance of the resonator changes accordingly. The impedance depends on the plasma characteristics, which depends on the magnetic field and absorbed microwave power, which will influence the position of the short-circuit plate. The graph in figure 4.13 depicts the position of the short-circuit plate when the resonance is found in the case where the plasma resistance is infinite.

The micro cap program was used to analyze the effect of various parameters on resonance. The results of the two calculations are depicted below. When the plasma resistance is $< 10^5\ \Omega$ the resonance is broad (see figure 4.15 and 4.16). The opposite is true when the resistance of the plasma is $> 10^5\ \Omega$ (figure 4.17 and 4.18). When the resistance is $2.5 \times 10^4\ \Omega$, the calculated power inside the resonator is equal to 30 W.

The co-axial cable plays an important role. Its length is 1.26 m which is equal to 5.32 λ. By changing this length, the resonance shifts, and to bring the resonance back to its original frequency the position of the short-circuit plate must be changed. This means that the length of the two co-axial lines T_1 and T_2, as indicated in the diagram figure 4.15 should be changed to obtain resonance at the same frequency.

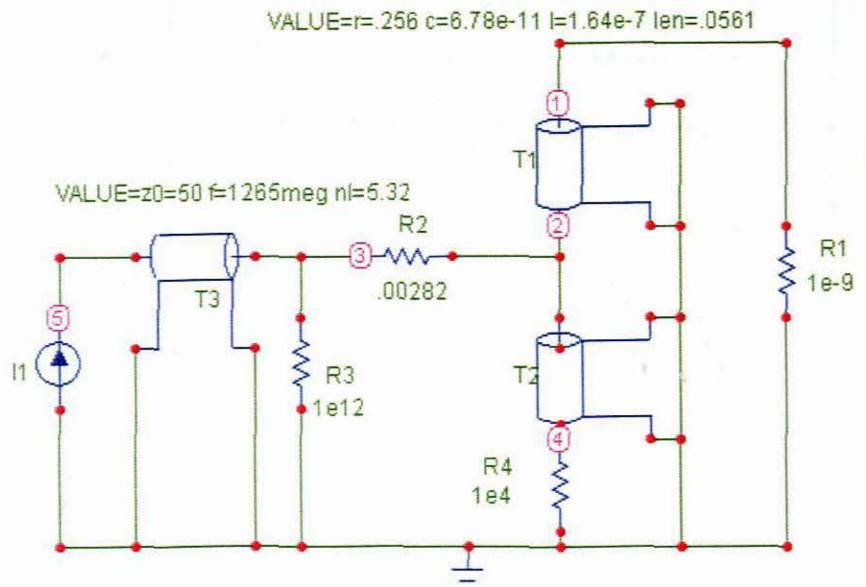

Figure 4.15: The circuit diagram as drawn with computer program Micro-cap program for a co-axial line length of 5.32 λ. The plasma resistance is assumed to be 10 kΩ.

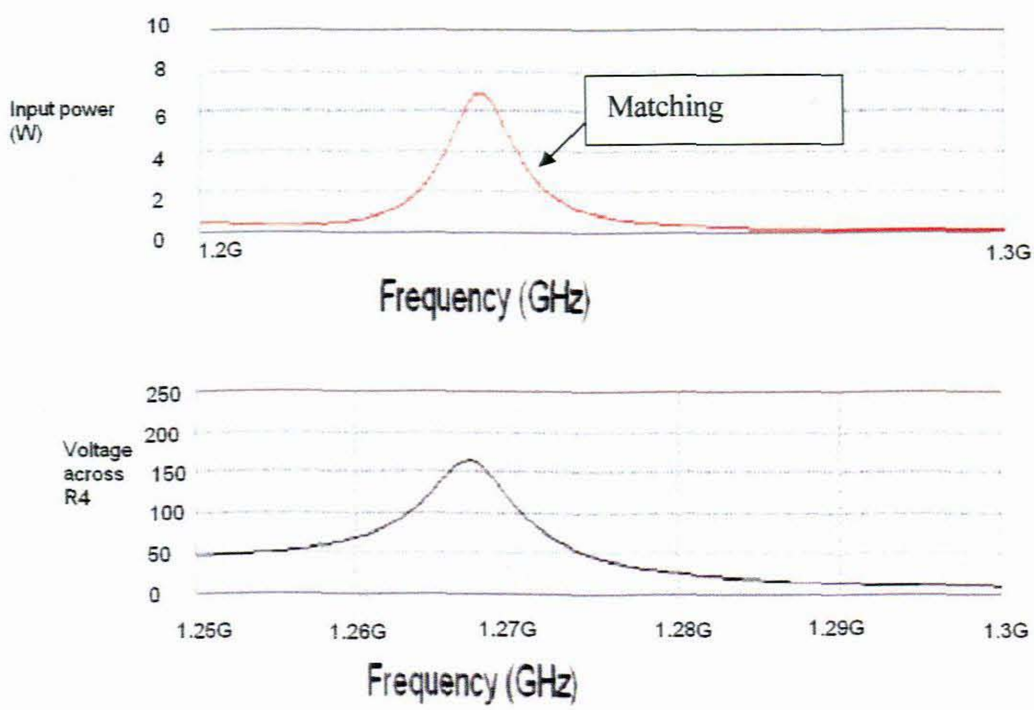

Figure 4.16: These graphs show the power dissipated in the source and the voltage assumed across the plasma chamber as a function of frequency of the power generator. The co-axial line length is 5.32 λ.

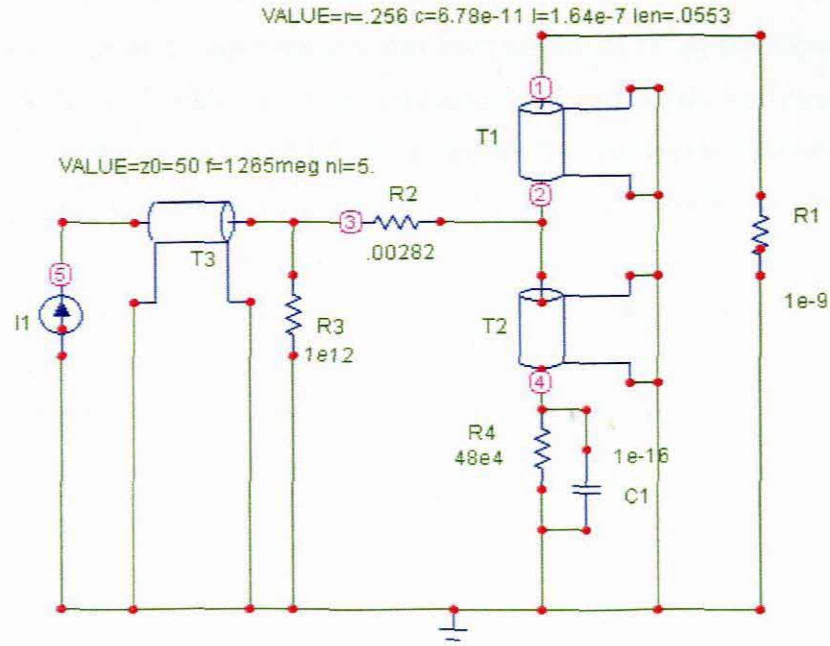

Figure 4.17: The circuit diagram for the co-axial line length of 5.0 λ. The plasma resistance is assumed to be 500 kΩ in parallel with a capacitance.

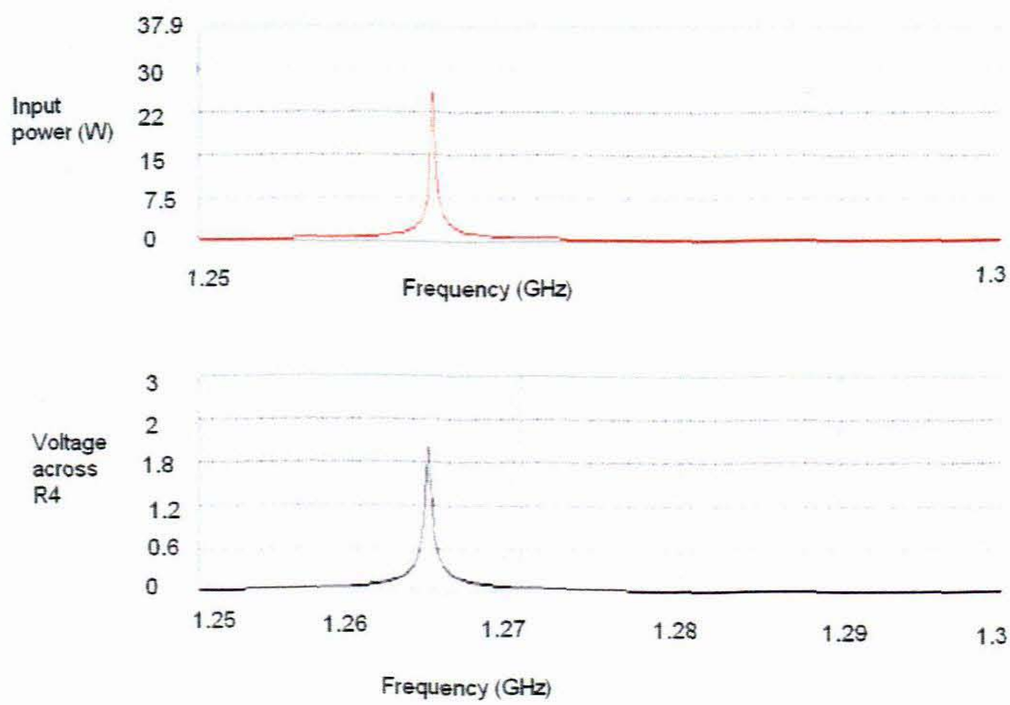

Figure 4.18: These graphs show the power dissipated in the source and the voltage assumed across the plasma chamber as a function of frequency of the power generator. The co-axial line length is 5.0 λ.

4.1.5 Plasma production in the source

The microwave ion source operates at a very low pressure of 10^{-4} to 10^{-7} mbar and the collision frequency of electrons with neutral atoms and ions is very low compared to the microwave frequency. Therefore this allows the continuous acceleration of electrons by the microwave electric field, which results in high electron temperatures.

A single impact energetic electron is used to raise the neutral atoms or molecules to ionization. Therefore, to obtain a high proton beam current, a high electron density of the plasma, a correct magnetic field and vacuum pressure as well as a high electron temperature are required **[Mok02]**. This is the case since the ion saturation current is proportional to the product of the plasma density and the square root of the electron temperature **[Bro89d]**.

4.1.6 Particle distribution in the plasma

The energy, velocity and temperature distributions of the particles in the plasma are very important parameters that should be taken into consideration. If there are no external forces, then the plasma will be in thermal equilibrium and therefore it would have particles with different velocities. The velocity distribution is described by Maxwell equation which is as follows **[Bro04]**.

$$f(u) = n\left(\frac{m}{2\pi KT}\right)^{3/2} \exp\left[\frac{-1mu^2}{2KT}\right]$$

Where

$f(u)$	=	distribution function
n	=	density, in particles per cm^3 and is given by
		$n = \int_{-\infty}^{\infty} f(u)du$
$f(u)du$	=	number of particles per cm^3 with velocity u and $u + du$
m	=	mass of the atom
T	=	plasma temperature
K	=	Boltzmann's constant
	=	$1.38*10^{-23}$J/K
$\frac{1}{2}mu^2$	=	kinetic energy of the particles

In one dimension this distribution equation becomes

$$f(u) = n\left(\frac{m}{2\pi KT}\right)^{1/2} \exp\left[\frac{-1mu^2}{2KT}\right]$$, where $f(u)$ describes the velocity distribution of the particles inside the plasma. The plasma temperature T gives the width of the distribution since it is possible to have ions and electrons with different Maxwellian distributions with different temperatures T_i for ions and T_e for electrons. This results from the different collision rate between particles.

The Maxwellian distribution of energy is given:

$$f(E) = f(u)\frac{du}{dE}$$

$$= n\left(\frac{4}{\pi}\right)^{\frac{1}{2}} (KT)^{-3/2} E^{1/2} e^{-E/KT}$$, where the mean energy is

$$\bar{E} = \frac{3kT}{2}$$ **[Bro89a, Hil]**.

The distributions of the gas particles in the plasma chamber can be represented in the form of a graph as shown in figure 4.19 using the Maxwell equation. For this calculation a typical electron energy kT_e = 1 eV is assumed and $f(u)$ is normalised to the density.

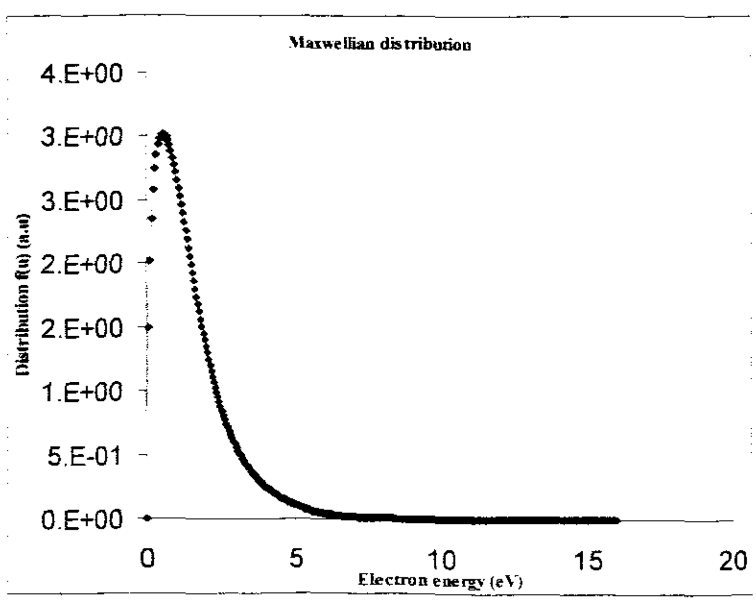

Figure 4.19: The Maxwell distribution of electrons in a plasma

Figure 4.19 shows that the probability of having many electrons for ionization at the ionization energy (15 eV) is very small. The contrary is true for electrons at about 1 eV to about 4 eV. At about 6 eV to 15 eV the current that could be produced is small due to the small amount of electrons available for ionization. Therefore, a higher electron energy is favourable for higher currents. This is achieved by increasing the electro-magnetic field coupled to the plasma, which electric component accelerates the electrons to higher energies and in addition increases the electron temperature. Further more, the path length of the electron is increased by the magnetic field superimposing the RF field.

4.1.7 The magnetic field in the source

The magnetic field causes the electrons to rotate around the magnetic field lines with the angular frequency $\omega = e^*B/m$ **[Con00]**. B is the magnetic field, m the particle mass and e the charge of an electron. The path length of electrons is increased by the rotation of electrons in these fields which leads to an increase in beam current. The function of the magnetic field is also to confine the plasma to the plasma chamber.

The microwave discharge source exploits the principle of the off-resonance discharge to generate a low-temperature plasma that produces a 1^+ ion beam with high efficiency and low energy spread **[Sun98, Tay93]**. It differs from an ECR ion source because the electrons motion is not in resonance with the RF field. The difference in behaviour of the electrons motion between the two sources can be seen in the following diagrams.

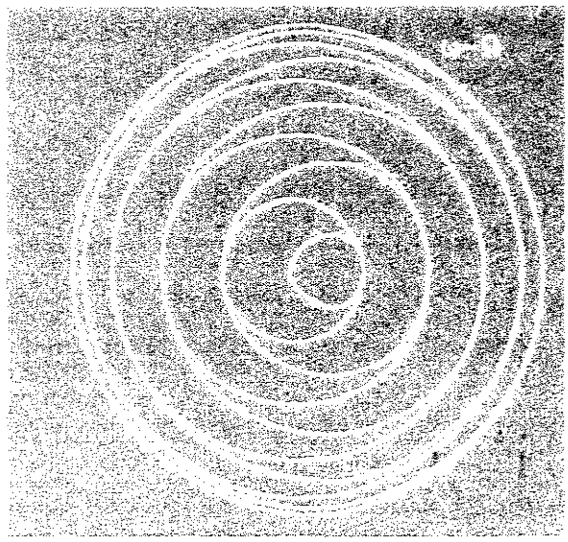

Figure 4.20: The off-resonance motion of the electrons in the magnetic field

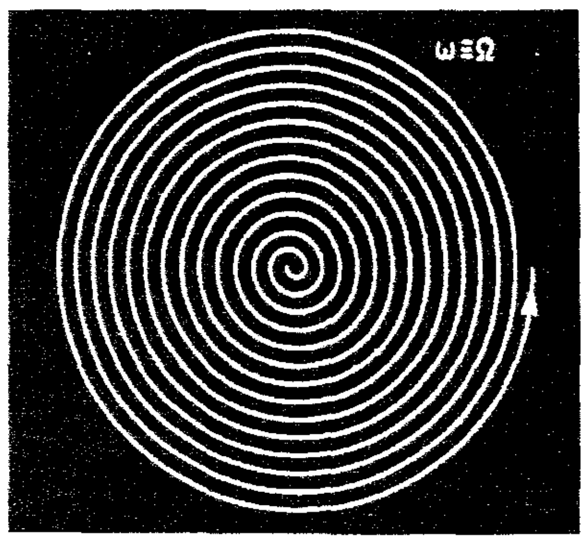

Figure 4.21: The resonance motion of the electrons in the magnetic field

The above figures 4.21 show the motion of the electrons inside the magnetic field. The electron motion is in resonance with the RF field and figure 4.20, the motion of an electron is off-resonance.

4.1.8 The ionization process in the plasma

Plasma is a gaseous body of ions, electrons and neutrals atoms of a certain density. In a discharge chamber at a low gas pressure the absorbed microwave power heats up the electrons. Electrons are accelerated by the electric field of the microwave to energies sufficient to cause ionization when they collide with molecules and atoms. In the collision process more free electrons are created and the discharge grows.

A certain minimum energy of the electron-atoms collision is needed for ionization to occur. In general the electron energy **[Mok02]**, E_e, must exceed the energy needed to remove the outermost bound electron from the neutral atom, called the ionization potential $\o$, with $E_e > e\o$; i.e., the energy required to remove the first electron from the atom.

The ionization potentials for most gases are in the vicinity of 15 eV (helium 24.6 eV) while typical gaseous discharge plasma electron temperatures are 1-10 eV. Thus most of the ionization that occurs is due to electrons in the tail of the Maxwell energy distribution (see figure 4.19).

Beside that, multi-step ionization in which the atoms, molecules are first excited into a higher energy level, which reaches the final ionization energy can take place. Some of the different processes are **[Con92, Hil]**:

- $H_2 + e \Rightarrow H + H + e$

  An energetic electron dissociates a H_2 molecule.
- $H + e \Rightarrow H^+ + 2e$

  An energetic electron ionizes an H atom (see figure 4.22).
- $H_{(2)} + e \Rightarrow H_{(2)}^* + e$

  An electron excites an H atom or an H_2 molecule.
- $H_{(2)}^* + e \Rightarrow H_{(2)}^+ + 2e$

  The excited H^* atom or an H_2^* molecule is ionized by an electron.
- $H_2 + e \Rightarrow H_2^+ + 2e$

  An energetic electron ionizes a H_2 molecule.
- $H_2 + H_2 \Rightarrow H_3^+ + H + e$

  The collision of two H_2 molecules leads to the formation of an H_3^- ions and an H atom.
- $H_3^- + e \Rightarrow H^- + H_2 + e$

  An energetic electron dissociates an H_3^- ion into an H^- ion and an H_2 molecule.

Note that these are the favoured reaction channels beside many others.

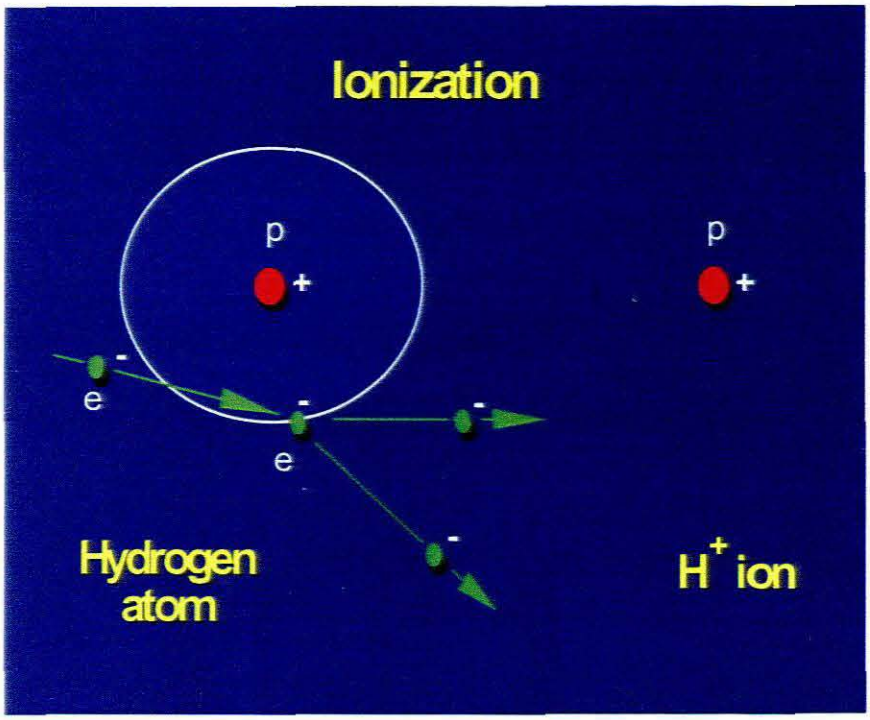

Figure 4.22: A picture showing the process of ionization **[Bot]**

Due to the magnetic field the ions (protons) and electrons spiral around magnetic lines. The radius of a proton's orbital motion in the magnetic field is given by:

$$\rho = .0014 \frac{\sqrt{AT_p}}{qB} (cm) \quad (4.6)$$

[Bro04]

with A the proton mass in a.m.u, q the proton charge in multiple of e, B the magnetic field in tesla and T_p the proton temperature in eV.

The radius for the motion of a proton with energy equal to the electron's ionization potential moving in the magnetic field of a ferrite magnet is very small. To concentrate the ionization close to the exit electrode, the plasma chamber should therefore be small.

It is also important that the frequency of an electron impact must be smaller than the applied microwave frequency otherwise the rotation motion of the proton or electron can not be sustained.

To increase the beam current, it is necessary to increase the ion density and the energy of the electrons by increasing the microwave power. This is obvious as the extracted current is given by:

$$J_p = en_p\sqrt{\frac{kT_e}{M}}.\exp(-.5) \tag{4.7}$$

with e the electron charge and M the proton mass.

4.1.9 The ion extraction process in the microwave ion source

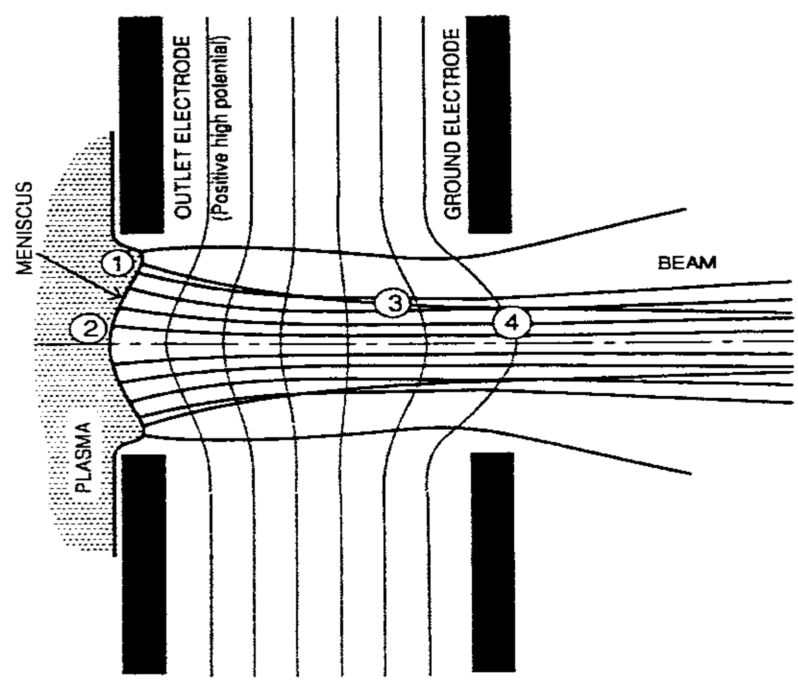

Figure 4.23: The extraction process of ions in the source **[Kel90]**

Extraction process takes place when a high voltage is applied between two electrodes, the outlet electrode and the ground electrode (see figure 4.23). The outlet electrode must be on the positive potential while the ground electrode is on ground potential. Factors that influence the beam quality in the extraction system are the applied magnetic field strength and also the space charge density of the resulting beam and the shape of the electrodes **[Kel90]**.

The emitting surface (meniscus see figure 4.23) acts as a boundary layer between the discharge plasma and the accelerated beam particles. The depth and the position of this layer with respect to the surrounding electrode depend on the densities of the plasma electrons and ions and their mobilities, which can be expressed in terms of temperature of the plasma **[Bro89b, Moko2]**. The extracted current is limited by the emission capabilities, geometry or space charge force. The extracted beam intensity can be calculated using the Child Langmuir law.

$$j = \frac{1}{9\pi}\sqrt{\left(\frac{2q}{m_i}\right)}\frac{V^{\frac{3}{2}}}{d^2}\text{, where}$$

j	=	current density in A/m^2.
V	=	extraction voltage in V.
q	=	ion charge in coulomb.
m_i	=	ion mass in kg.
d	=	acceleration gap width in m.

CHAPTER 5

EXPERIMENTAL WORK

5.1 Experimental setup

The experimental work has been carried out with two different setups. The first setup uses a 1.03 GHz microwave generator and the magnetic field is generated by the cylindrical shaped permanent magnet shown in figure 5.1. In the second setup the magnetic field is generated by an array of rectangular permanent magnets arranged as shown in figure 5.2, and the microwave frequency is 1.265 GHz. Preliminary calculations were done to determine the position of the short-circuit plate and the coupling point for operation at both frequencies. The ECR conditions of the magnetic field applied at these two frequencies are different. At 1.03 GHz the ECR condition of the magnetic field is 370 G while at 1.265 GHz it is 460 G. Figure 5.1 shows the magnetic field measurement setup for the cylindrical shaped magnets.

Figure 5.1: The magnetic field measurements.

Figure 5.2 shows the versatile magnet assembly which makes it possible to change the magnetic field and shape. The magnets are movable up and down and also in and out by turning the screw as can be seen in the drawing. This assembly allows only two bar magnets (12 x 10 x 40 mm) to be inserted in each of the eight blue sectors. The material from which the assembly is built up is non-magnetic. With this assembly the magnetic field of 1.3 kG at the center of the magnets was measured.

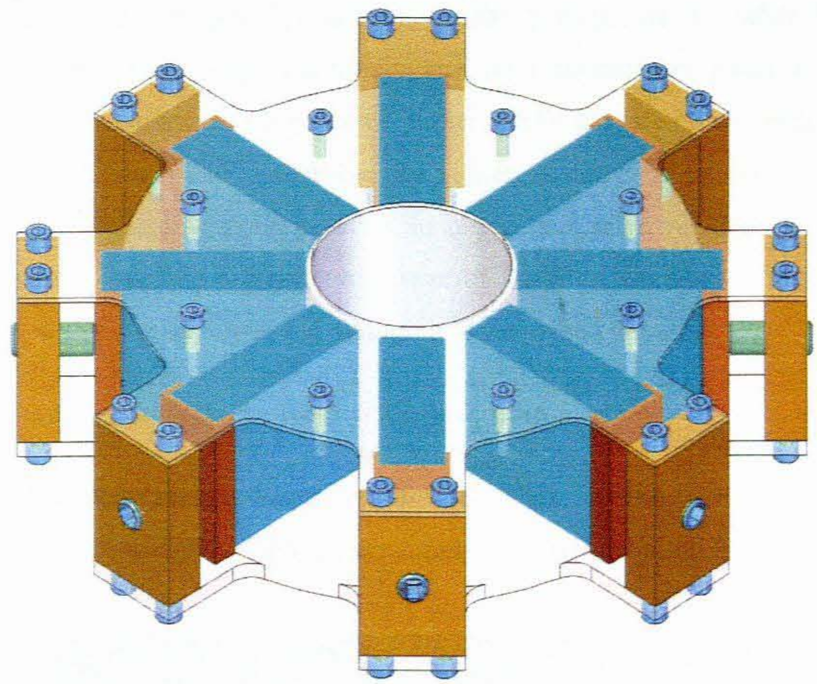

Figure 5.2: The final magnet assembly that was used for measurements.

The microwave ion source is mounted vertically on the test stand. It is on a high potential such that the beam is extracted downward and then bends 90 degrees in the vertical plane into the diagnostic chamber. The first Faraday-cup is placed at a distance of 10 cm behind the extraction system of the microwave ion source in the diagnostic chamber. The second Faraday-cup is placed 1.5 m behind the bending magnet. A metal ring, biased to -500 V, is placed in front of the faraday cup to suppress any electrons that might escape from the cup due to the ion beam impinging on the cup.

The bending magnet is used as the mass analyzer. At a specific current value of the bending magnet power supply, there is a specific species for hydrogen measured on the Faraday-cup. The energy of the beam can be changed by changing the extraction voltage.

5.2 Operating the source at 1.03 GHz

To ignite the plasma, the source, without the plasma is matched to the generator, at a power level of 5 W. The gas flow is set to reach a pressure of 10^{-4} mbar. When the power is increased plasma ignition is indicated by a current flow towards the outlet electrode and an increase in the reflected power. Next, the gas flow is reduced to its operational condition of 10^{-6} mbar and the source is tuned by means of the short-circuit plate and coupling point position to obtain minimum reflected power. This setup allows for coupling a maximum power of 20 W to the source. The setup for 1.265 GHz, with more sophisticated matching, is described next.

5.3 The connection with the 1.265 GHz generator

The new generator, using a frequency of 1.265 GHz, is shown in figure 5.3. The figure shows additionally the 24 V power supply, the circulator and the dummy load.

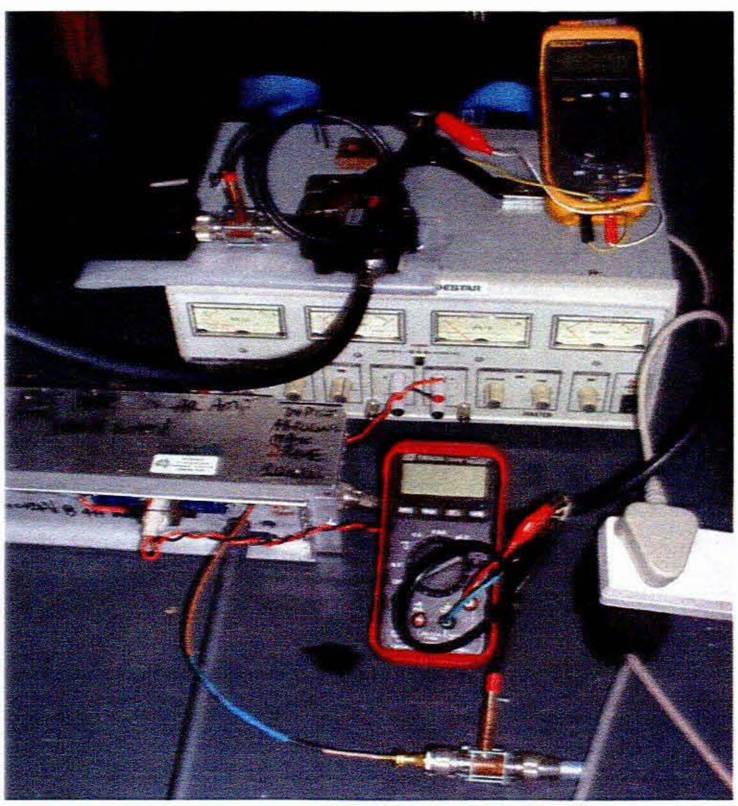

Figure 5.3: The connection of the microwave generator to the 24 V power supply. The dummy load is on the top left side in the figure.

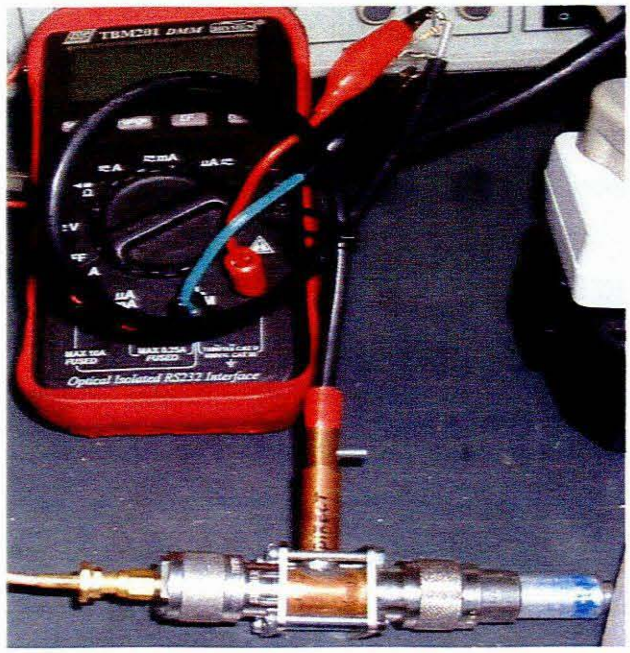

Figure 5.4: The directional coupler used to measure the forward power.

Figure 5.5 is a schematic drawing of the directional coupler mentioned in figure 5.4 and it shows the way in which the microwave diode D1 in the figure is coupled to the inner conductor of a co-axial cable.

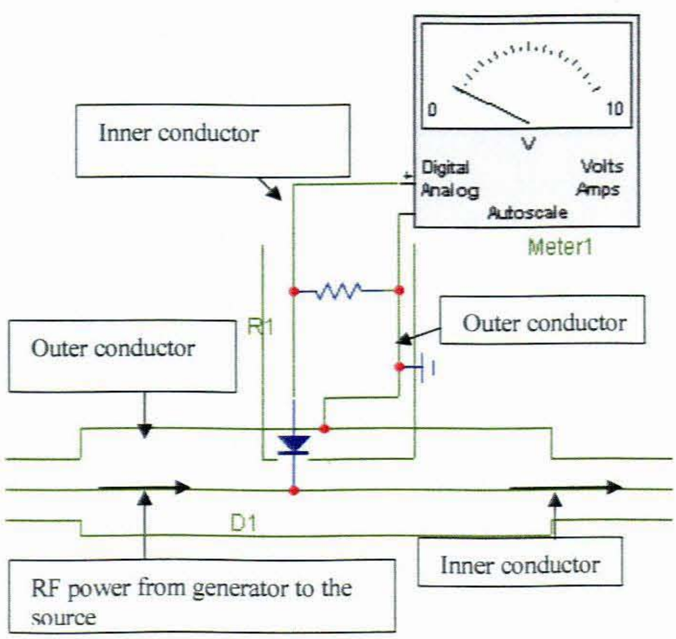

Figure 5.5: A schematic drawing of the photo in figure 5.4.

The signals proportional to the output and the reflected power are measured using a multimeter, a microwave diode (1N21F) and a 10 kΩ resistor. The diode rectifies the microwave and the DC voltage obtained across the resistor is measured. The diode is connected to the central core of a co-axial cable in series with the resistor, the latter being earthed. The cable provides the necessary capacitance for the detector.

A circulator is used to divert the power reflected from the ion source into the dummy load in order to protect the amplifier. The current between the outer conductor and outlet electrode of the source is measured to observe when plasma is formed. The current into a faraday cup is measured by reading the voltage across a 10 kΩ resistor, connecting the faraday cup to ground potential, using a multimeter on its most sensitive range. This gives a resolution of 0.1 μA. The 10 MΩ internal resistance of the meter introduces a negligible error.

5.4 Starting the source with the low cost solid state 1.265 GHz generator

The procedure of starting the source is as follows:

- Allow the gas to enter the source to increase the vacuum reading to the range of 10^{-4} to 10^{-3} mbar.
- Switch all voltmeters on.
- Switch on the 24 V power supply for the microwave generator.
- Increase the power output of the microwave generator to 30 W. The current through the power supply of 24 V will be > 3 A.
- Move the short-circuit plate up and down
- Move the microwave input point up and down
- The plasma will ignite when the correct matching has been found with both the short-circuit plate and input point. Ignition is clearly observed on the multimeters that measure the forward power in the source and the reflected power in the dummy load. The forward power should be at a maximum and the reflected power at a minimum.

The power indicated by the amplifier is not completely dissipated in the source due to losses in the circulator and the losses in the co-axial cable. The activity inside the plasma chamber is observed on a multimeter connected across the outer conductor and the outlet electrode indicating when the source is on.

- Diminish the gas flow to obtain a pressure of 5.0 x 10^{-6} mbar.

During the plasma ignition, mismatch will occur; therefore, the correct matching is required to bring the reflected power to minimum by tuning the short-circuit plate, trombone line and the coupling position, which automatically leads to an optimum beam intensity.

5.4 Effect of contamination

When any new part has to be installed it is important to clean it before installation to make sure that it's free from oil contamination that occurred during the machining stage in which cutting oil is used.

The cleansing is done for 30 minutes by dipping the new part into an ultrasonic bath full of alcohol which dissolves oil rapidly. If the part has been installed without being cleansed the beam of heavy masses increases to the detriment of the proton beam current. The table below shows the effect of heavy masses on the proton beam current.

Extraction voltage	**H^+ Beam**	**H_2^+ Beam**	**H_3^+ Beam**	**H_2O Beam**	**C**	**Condition of cleanness.**
2 kV	1.9 µA	7 µA	2.6 µA	1.28 µA	0.9 µA	**Contaminated**
2 kV	1.5 µA	6.3 µA	5.7 µA	1 µA	0.25 µA	**Not cleaned**
2 kV	4.6 µA	21.5 µA	19.6 µA	0.74 µA	0.06 µA	**Very Clean**

Table 5.1: Table showing the effect of the heavy materials on other beams.

5.5 Optimization of the source

The source is optimized by moving the short-circuit plate and the coupling point up and down until the reflected power is at minimum. Additionally, the gas flow should be regulated to change the gas pressure to a value of 10^{-6} mbar and move the trombone line up and down to the point where the reflected power is at minimum.

These parameters can iteratively be changed to optimize current into the first Faraday-cup.

5.6 Magnetic field in the microwave ion source

The magnetic field plays an important part in the production of ion beams. When the magnetic field is lower than the ECR field condition, $\omega_{ECR} > \omega$ the complex equation for the reflection index of the plasma for microwaves is imaginary.

This means that in theory all the microwave power wi!l be reflected. The reflected index gets a finite real value if $\omega > \omega_{ECR}$ **[Bro04]**. This is the reason why the magnetic field of this type of source should be larger by 30% than the field that would sustain the ECR condition.

The way in which the geometry of the plasma chamber and outlet electrode is made as well as the correct positioning of mild steel is necessary to shape the flux lines to focus the electrons around the outlet electrode **[Bro04]**.

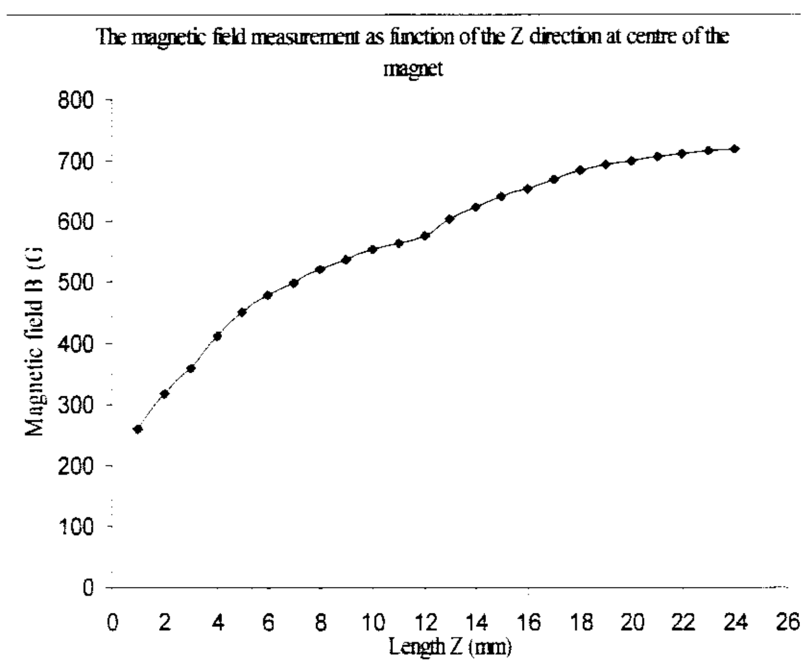

Figure 5.6: A graph of the measured magnetic field at the centre of the magnet in the microwave ion source. The 12 mm plasma length lies between 14 mm to 26 mm on the horizontal scale.

In view of this importance the magnetic field is measured. The apparatus, shown in figure 5.1, for measuring the magnetic field is a cylinder of plastic with square slits at various positions inside the plastic in which a probe is inserted. This cylinder fits inside the magnet with the outlet electrode, made of a mild steel, at its correct position. Figure 5.6 shows the field as a function of the z-axis of the magnet measured on the central line for the 1.265 GHz source.

Figure 5.7 shows the magnetic field measured using the magnet assembly shown in figure 5.2. With this magnetic field the highest proton beam of 26.7 μA was measured.

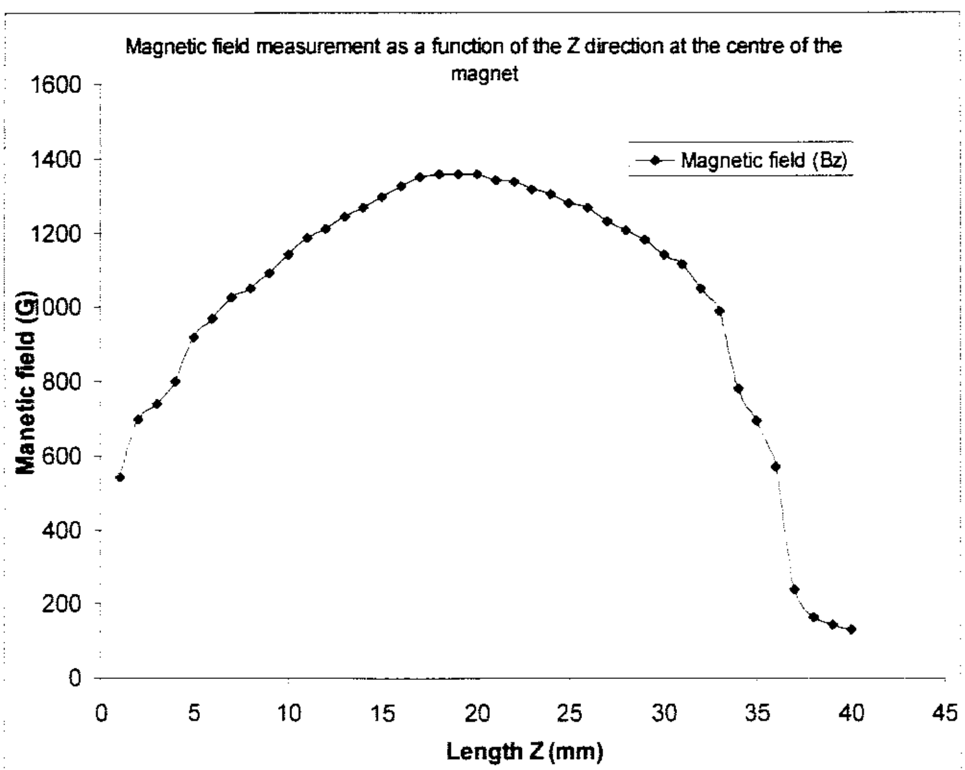

Figure 5.7: Results of the magnetic field measurement obtained from the magnet assembly of figure 5.2. The 7 mm plasma length lies between 28 mm to 35 mm on the horizontal scale.

CHAPTER 6

RESULTS AND DISCUSSIONS

6.1 Results and discussions

The properties of the ion species extracted and values of the bending magnetic field are shown in the table 6.1 at an extraction voltage of 6 kV.

Extraction V (kV)	6		
Ion species	H^+	H_2^+	H_3^+
B_{rho}	0.011192625	0.015830904	0.0193897
Q	1	1	1
T (MeV)	0.006	0.006	0.006
E_0 (MeV)	938.2588474	1877.028689	2815.7985
E_0/938.259	1.00	2.00	3.00
M_0 (ame)	1.0078252	2.0156504	3.0234756
90^0 Bending magnet			
B (T)	0.05202	0.07357	0.09011
I (Amp)	2.2	3.2	3.9

Table 6.1: The table for comparison of the ion species for the ion source

The spectrum of the beam as a function of the current through the bending magnet is shown in figure 6.1. This spectrum was obtained at a frequency of 1.03 GHz. It shows that the proton beam is very small compare to both the H_2^- and H_3^-. During the experiment it is observed that when the H_3^+ beam decreases the H^+ and H_2^- beam increases and vice versa. This is due to the recombination **[Eis05]** of H^- and H_2^+ with unionized hydrogen molecules in an ion source according to the following reactions:

$$H^- + H_2 <= H_3^-$$

$$H_2^+ + H_2 <= H_3^- + H$$

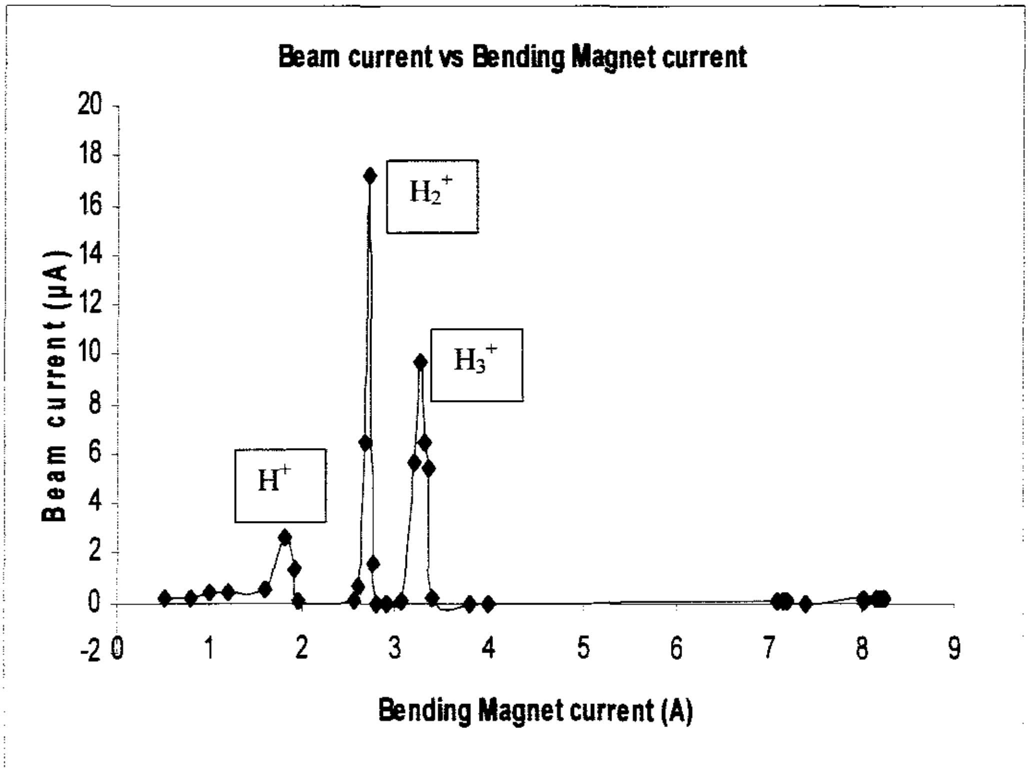

Figure 6.1: The beam spectrum obtained at a frequency of 1.03 GHz

6.2 Optimization by changing the cathode material and design

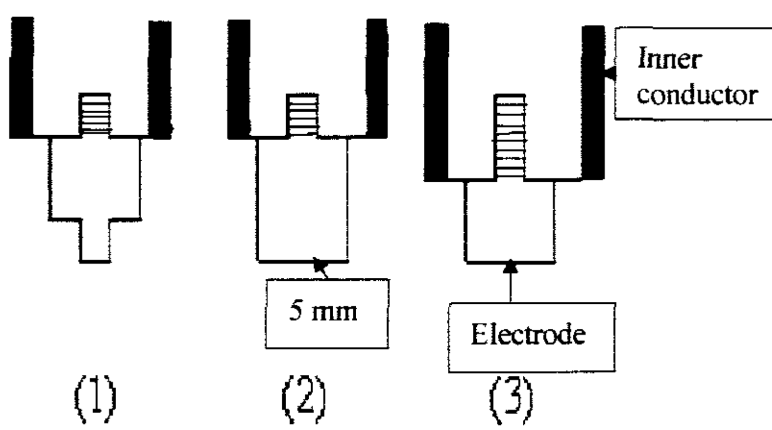

Figure 6.2: The different types of electrodes used in the source are numbered as (1), (2) and (3), respectively. The top parts of each of these electrodes were screwed into the inner conductor.

Different electrodes are used with various shapes and material (figure 6.2). The copper electrode produced the highest proton beam intensity. The aluminium electrode was proposed but never used in the source.

These electrodes have a 1 mm diameter hole through which the gas can be injected into the plasma chamber. They are screwed into the inner conductor.

The electrode named (1) in figure 6.2, is made from copper and another from steel. With the copper electrode the proton beam intensity of 23.3 μA is produced but with the steel electrode only 9 μA was measured. The proton current produced using (2) and (3) was 1.6 and 1.9 μA, respectively with a conical Al outlet electrode. Therefore (1) was recommended to be used in the source.

6.3 Optimization of the source by changing the plasma chamber length

To increase the plasma density at the outlet aperture the plasma chamber length was reduced. Changing the plasma chamber length causes an increase in beam intensity because of the shorter distance from ionization to extraction. It also enhances the plasma density since the shorter the plasma chamber the denser the plasma near the outlet electrode.

The plasma produced by the 12 mm long plasma chamber produced the highest proton beam, and relative lower H_2^+ and H_3^+ beams but the 15, 18, 22 mm long chamber produced lower H^+ and relative higher H_2^+ and H_3^+ beams. The plasma chamber length was further reduced to 9 mm but the proton intensity was decreasing while H_2^+ and H_3^+ were increasing (see figure 6.3). This was due to the short distance for the ionization to completely take place. Therefore the 12 mm plasma chamber length is recommended to be used. A graph of the beam current versus the plasma chamber length is shown below in figure 6.3.

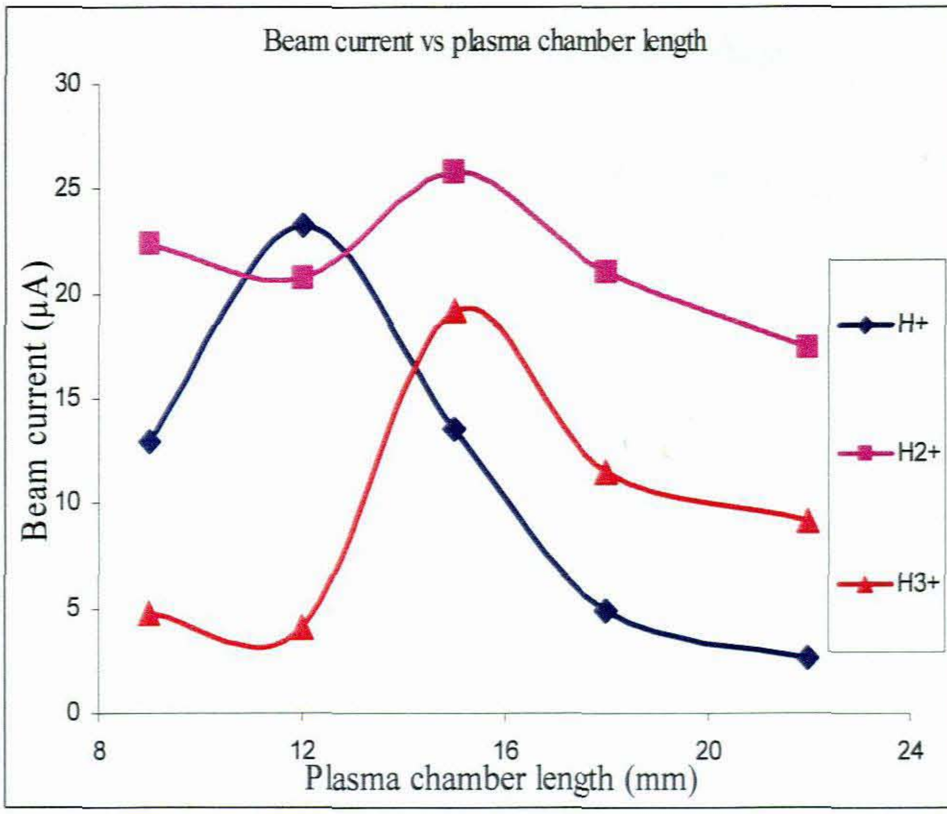

Figure 6.3: A graph of the behaviour of the beam current as a function of the plasma chamber length

6.4 Optimization of the source by varying the extraction voltage

The production of beam depends on the acceleration voltage. The acceleration voltage was changed from 2 kV to 6 kV in steps of 0.5 kV and the output beam current was observed to decrease. The best beam current was obtained at the acceleration voltage of 3.5 kV and at the vacuum pressure of 6.6 x 10^{-6} mbar. The graph of beam current versus extraction voltage is depicted below in figure 6.4.

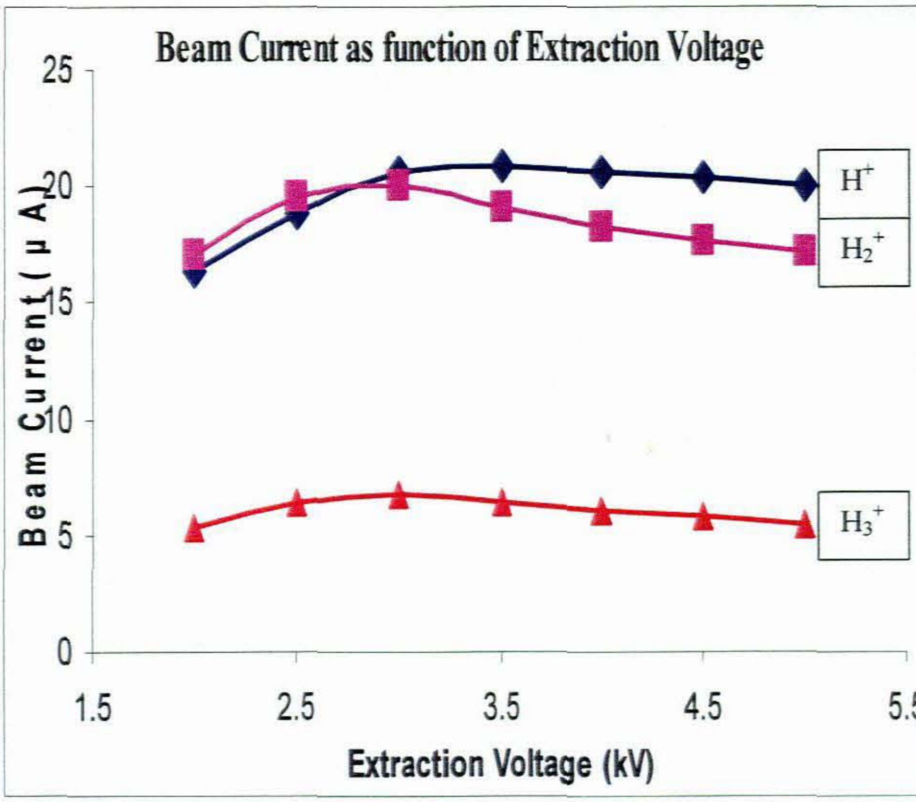

Figure 6.4: A graph of the behaviour of the beam current as a function of the extraction voltage. The pressure was 6.6 x 10^{-6} mbar and the outlet electrode used is Al and is conical in shape.

The highest beam current at a specific extraction voltage depends on the vacuum pressure. If the vacuum pressure is kept constant and the extraction voltage increases the beam current will reach a maximum, becomes constant or drops. To optimize the current the vacuum pressure will need to be varied. Figure 6.4 shows that the H^+ beam current increases as the extraction voltage increases but it will reach a maximum where it becomes constant. As the extraction voltage continues to increase it then drops due to over focussing. The beam current for H_2^+ and H_3^+ increase up to the point, where the extraction voltage reaches 3 kV and then drops as the extraction voltage continue to increase.

6.5 The optimization of the source by changing the extraction system

Because the shape of the electrical and magnetic field play a great role in the intensity of the beam current produced, an investigation was done by changing the shape and material of the extraction system. The steel outlet electrode was changed to aluminium and the shape from a flat surface to a conical one.

The aperture on the outlet electrode was changed from 0.45 mm to 1mm diameter and the aperture on the ground electrode was decreased from 7 mm to 4 mm. The changes shows that the use of a steel outlet electrode is not so good but the use of the aluminium shows an increase in beam current produced. The table below shows the result of both the steel and aluminium outlet electrode. The dimension of the conical part of above the flat surface is 5 mm.

Figure 6.5: A pictures of the outlet electrode for different materials and shapes. The electrodes from left to right are: conical mild steel, flat mild steel and conical aluminium.

Outlet electrode	H^+	H_2^+	H_3^+
Flat steel electrode	3	17.9	15
Conical steel electrode	9	19	5.6
Conical Al electrode	23.3	20.7	4.2

Table 6.2: The beam current measured using outlet electrodes of different shapes and materials. The ground electrode in the last case was made of mild steel.

The results depicted in the above table were obtained using the stronger magnetic field of 1.3 kG, a 12 mm plasma chamber length and an extraction voltage of 3.5 kV. These results show that outlet electrode made out of aluminium gives the best results.

This behaviour is possibly related to a higher secondary electron emission coefficient of the aluminium electrode.

Optimizing the source by opening the aperture on the outlet electrode from 0.45 mm to 1mm aperture diameter and decreasing the size of the aperture on the ground electrode from 7 mm to 4mm in diameter, respectively, increased the beam on both the first faraday and second faraday cup. At an aperture diameter of 0.45 mm and 1 mm the plasma density of 0.63 mA / cm^2 and 2.9 mA / cm^2, respectively, was calculated.

6.6 The simulation of the extraction system using IGUN

IGUN (Ion Gun) **[Bec92]** is a two-dimensional ray tracing code that has been developed for simulation of the extraction of positive ions from plasmas. It solves the Poisson equation iteratively assuming cylindrical symmetry. Space charge effects are included.

A pre-processor, GPED (Graphic Polygon Editor) is used to set up the boundary conditions, including the definition of internal electrodes, dielectric boundaries, and slanted Neumann boundaries (field lines as boundary elements). The boundary input is mesh independent and can use any coordinate system from a drawing.

The program's outputs are equipotentials lines and particle trajectories. From the latter the rms beam parameters are calculated. Figure 6.6 shows the results obtained during the simulation of the extraction system using IGUN program. This is the extraction system we used to obtain our final result.

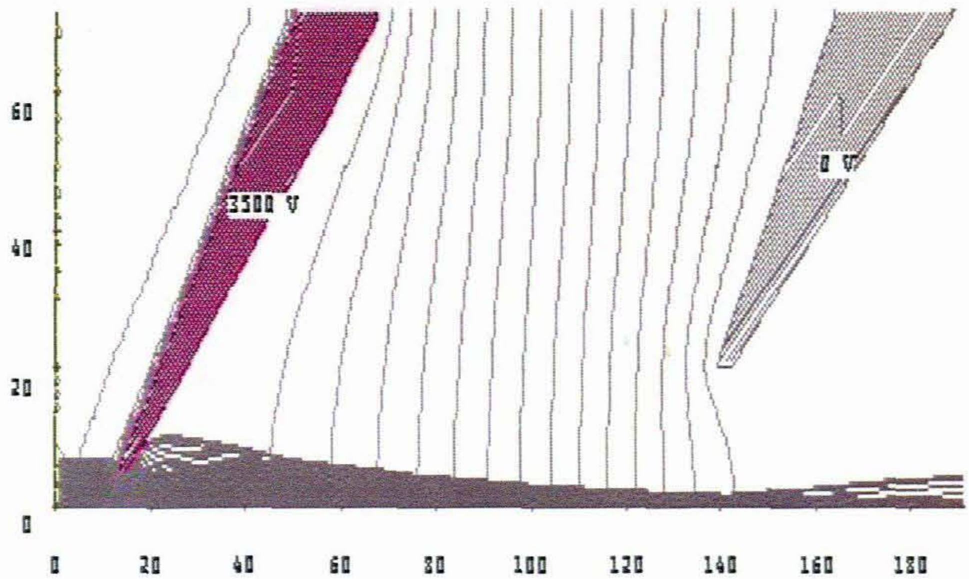

Figure 6.6: The simulation of the extraction system. The beam envelope can be seen near the x-axis.

6.7 The optimization of the source by applying voltage across the source

The graph, figure 6.7, shows how the beam behaves when a voltage is applied across the outer conductor and outlet electrode. The applied voltage was increased in steps of 10 V and the extraction voltage was kept constant at 2 kV. The results show that applying the voltage does not help to increase the proton beam current. The graph shows that the biased outlet electrode does not have any influence on the output beam intensity in the range investigated.

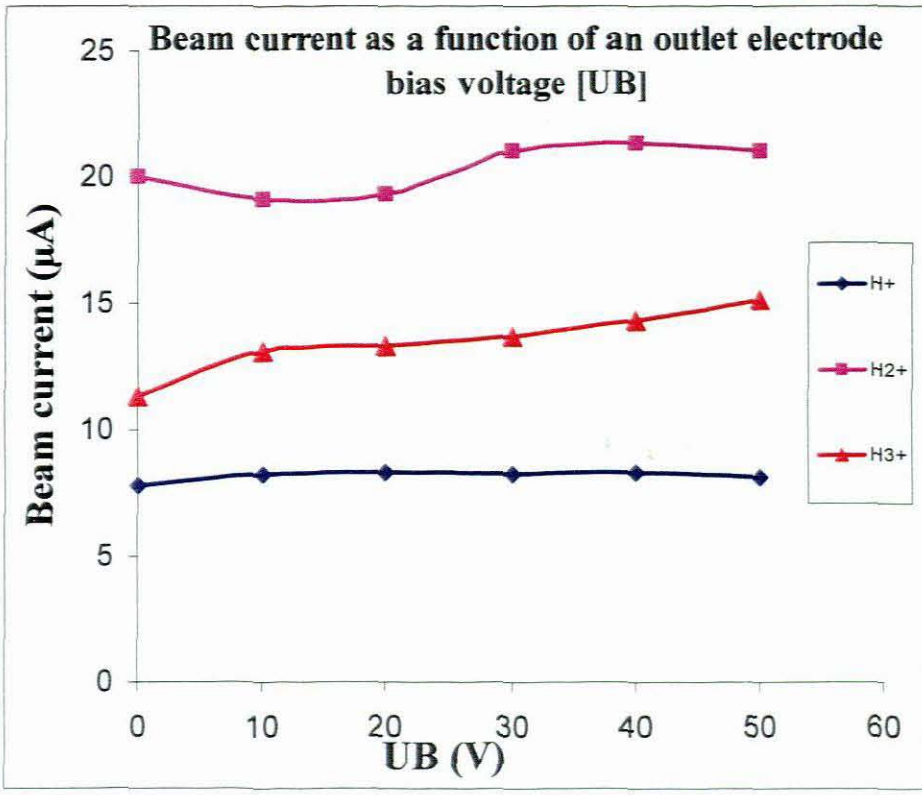

Figure 6.7: This graph shows the behaviour of the beam intensity when a bias voltage is applied across the outer conductor and outlet electrode.

6.8 The optimization of the source by changing the magnetic field

The two sets of three 12 mm ferrite magnets (refer to figure 5.1) were used in the source for the confinement of the plasma. One of the sets has a weaker field of 717 G (on the surface) and the other a stronger magnetic field of 1086 G (on the surface). The beam current was smaller when the weaker magnets were used in comparison with the stronger magnets. For detail about the field of the later magnet assembly used refer to section 5.7.

6.9 The optimization of the source by changing the gas pressure

The graph, figure 6.8, shows the effect of the gas pressure on beam current. To obtain the optimum beam current it is necessary to retune the position of the short-circuit plate, the coupling point and the slide of the trombone line. This was done to obtain the graph in figure 6.8.

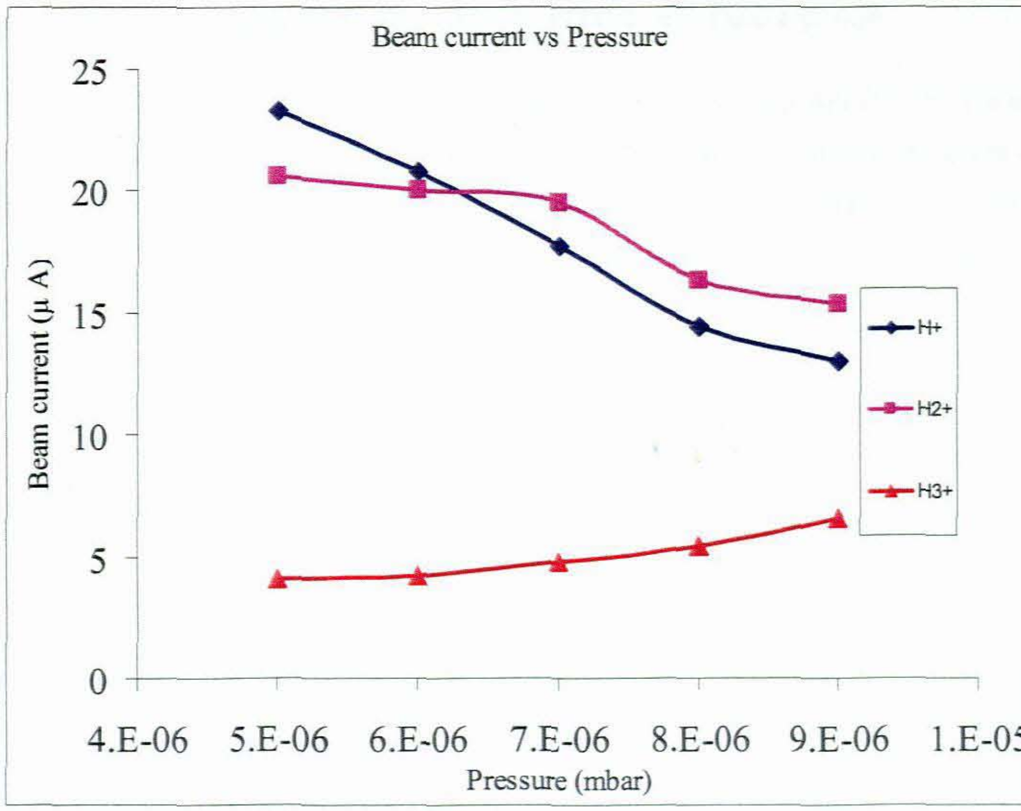

Figure 6.8: The graph showing the dependence of the beam current on the pressure

The above graph shows that as the pressure increases the beam intensities of H^+ and H_2^+ decreases, but the H_3^+ intensity increases since the reaction $H^+ + H_2$ is more probable when more H_2 molecules are available. This graph shows that this source operates at a low vacuum pressure and the gas consumption is therefore low. For lower pressures than 5 x 10^{-6} mbar the plasma generation becomes unstable. The pressure was measured at the diagnostic chamber.

6.10 The optimization of the source by changing the frequency

The optimization of the source was done at various frequencies namely: 1.03 GHz and 1.265 GHz. The beam intensity produced using the 1.265 GHz generator and the plasma chamber with length 22 mm and 12 mm produced higher beam intensities than using 1.03 GHz generator. Both frequencies operated in the weaker and stronger magnetic field but the beam produced at 1.265 GHz was higher than that of 1.03 GHz. Therefore the higher frequency of 1.265 GHz is recommended to be used to obtain much higher beam current for the same microwave power of 30 W.

6.11 The optimization of the source by increasing microwave power

The proton beam can be increased by increasing the microwave power into the source. There is a limit to this because the source becomes hot. Figure 6.9 depicts the graph of the beam current as a function of the microwave power. The intensity of the H^+ increases while the beam intensity of the H_2^+ and H_3^+ stay constant. The extraction voltage was 3.5 kV.

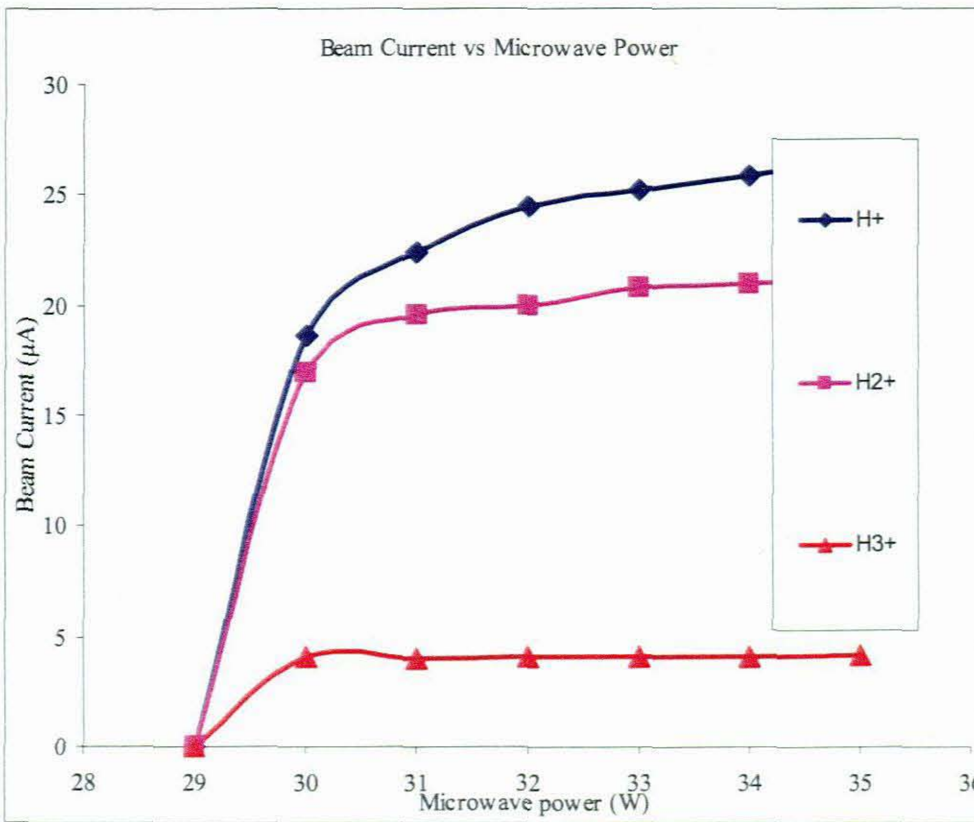

Figure 6.9: The graph that shows the dependence of the beam current on the microwave power.

6.12 The optimization of the source by changing the trombone line length, position of the short-circuit plate and the microwave input point position

Optimizing the source by changing the position of the trombone line, short-circuit plate and coupling point increases the beam current on the first Faraday-cup and second Faraday-cup depending whether the resonance is still maintained.

The graph, figure 6.10, shows the beam spectrum obtained at an extraction voltage of 3.5 kV and a pressure of 5 x 10^{-6} mbar. This graph was taken at a frequency of 1.265 GHz. In the figure it is clear that the intensity of the protons beam is the highest. The beam current for H^+, H_2^+ and H_3^+ are 23.3 μA, 20 μA and 4.1 μA, respectively. Comparing the graphs 6.1 and 6.10 it is clear that there was an enormous improvement of the beam intensity during the course of this study.

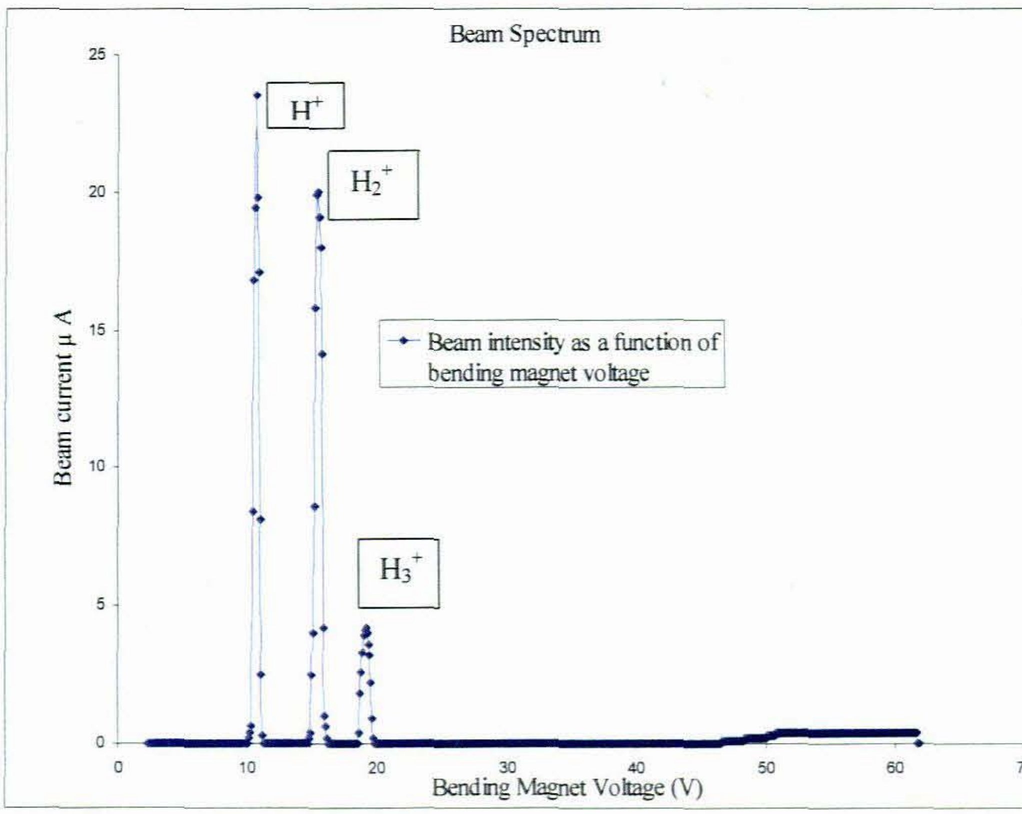

Figure 6.10: The beam spectrum of the source. The x-axis is given in voltage instead of current because the readout of the voltage was more sensitive.

6.13 Comparing the microwave ion source and the duoplasmatron ion source

The graph in figure 6.11 shows the beam current for various ions in the duoplasmatron source that is used in the Van de Graaff accelerator. It is evident that this source uses various power supplies that are absent in the microwave ion source. Adding the power consumption of these components together plus the power for the solenoid coil, a value for the total power consumed is nearly 200 W.

The maximum beam intensity for the H^+ is 30 μA that is 9% higher than the value for the microwave source. It is also evident that the gas consumption is higher than that of the microwave source. The microwave ion source has therefore a big advantage to be used in the environment of the Van de Graaff. There is no cooling or filament needed, and the power and gas consumption are low. The beam current produced is somewhat lower, but it can still be increased by increasing the microwave power. The graph below, figure 6.11, depicts how the beam current from a duoplasmatron ion source depends on the vacuum pressure **[Eis05]**.

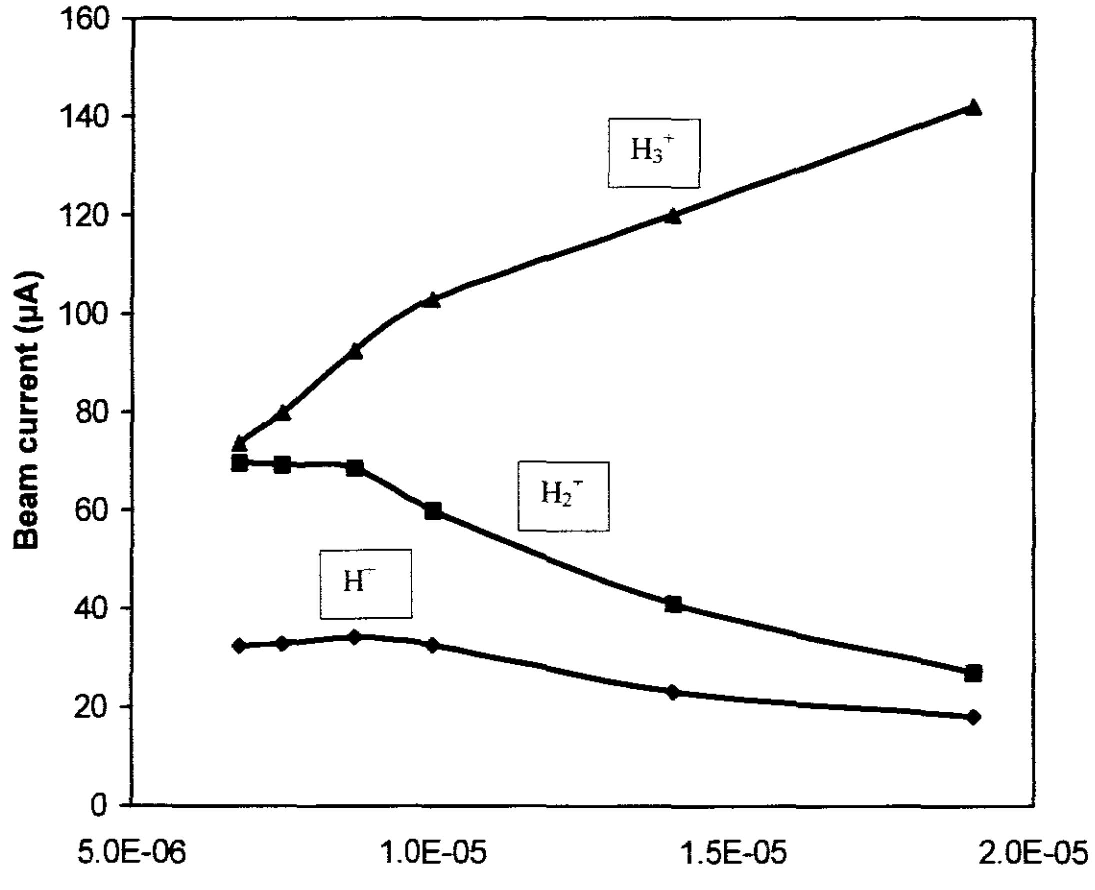

Figure 6.11: Measured beam current for different Hydrogen-ion species as a function of the pressure in the beam line of the ion source test bench, for the hot-cathode duoplasmatron ion source, operated under the following conditions: arc current = 1 A, filament current = 25 A, extraction voltage = 5 kV. The arc voltage decreased from 97 V to 81 V as the gas flow to the source was increased **[Eis05]**.

CHAPTER 7

SUMMARY AND CONCLUSIONS

7.1 Conclusions

In the course of the work for this thesis a microwave ion source for the production of H^+-ions was designed, built, and successfully tested. The requirements for the source are determined by its application in the 6 MV Van de Graaff accelerator at iThemba LABS. The source dimensions have to be small to fit in the accelerator's high voltage terminal. It should have an uncomplicated mechanical design, e.g. no water cooling, the electrical design should need only a small number of power supplies, and the source should have low power consumption. Furthermore, beams from the source should be easily reproducible and the source must be reliable with few break-downs. It should start easily and the electrodes lifetime should preferably of the order of few weeks.

These requirements could be fulfilled by developing a miniaturized source chamber in which the plasma is excited by microwave energy. The microwave amplifier used for the initial tests was borrowed from the polarized proton source at iThemba LABS. It is adjustable in frequency from 1 to 2 GHz. Some tests were done between 1 and 1.2 GHz but most were done at 1.03 GHz. A low cost 30 W solid state amplifier, normally used in amateur communications, was purchased for further tests. It has a fixed frequency of 1.265 GHz which coincides with the highest practical frequency of our ($\lambda/4$) quarter wave resonator for the source. Furthermore, the chamber dimensions required a special design of the microwave resonator and matching section. By using a movable short-circuit plate, it is possible to use the resonator over a range of frequencies (1 to 1.3 GHz) and provide an impedance matching. Permanent magnets surrounding the source chamber ensure effective plasma confinement. The magnet assembly using an array of CoSm magnets as shown in figure 5.2 was used to enable an easy change of a field profile and strength. The range at the centre of the magnet lies between 0.03 T and 1.3 T. This can be done without breaking vacuum in the source.

The optimization of the source performance was mainly done by investigating the influence of the plasma chamber's longitudinal dimension and the magnetic field configuration. It was found that a short plasma chamber, 12 mm long, in combination with a strong longitudinal axial magnetic field of 0.12 T and a conical outlet electrode made out of aluminium (giving a plasma of 7 mm long) results in the highest atomic ion current and lowest current of accompanying molecular ions. The extraction system was kept constant because the main aim was to improve this source.

With a microwave power of 30 W an H^+ current density of 3 mA/ cm^2 is achieved which results in an extracted and analyzed H^+ current of 26.7 μA for an outlet electrode aperture diameter of 1mm. In this configuration the ion source ignites easily and delivers a stable beam at low gas consumption. The only parameter to be adjusted after ignition is the gas flow and the position of the short-circuit plate.

The achieved current of 26.7 μA for protons is comparable to that obtained from the existing duoplasmatron ion source. Due to the fact that the microwave ion source has distinguished advantages with respect to operation and reliability over the duoplasmatron, it will be worthwhile to develop a production version which can be tested in the accelerator.

APPENDIX

The K-value of a Cyclotron

The limitation by the magnet of a cyclotron to the maximum attainable kinetic energy T in MeV for a particle with mass A and charge Q in terms of the proton mass and proton charge, respectively, can approximately be written in the form:

$$T = K \frac{Q^2}{A}$$

It is shown below that the constant K is given by:

$$K = 47.89B^2R^2$$

with B the maximum average magnetic flux density of the magnet on the extraction orbit in tesla and R the average extraction radius.

In the following:

v is the speed of the particle with kinetic energy T in joule

γ is the ratio of the total energy to the rest energy of the particle

m is the mass of the particle in kg

q is the charge of the particle in coulomb

β is ratio of the speed of the particle to c, the speed of light in vacuum

E_0 is the rest energy of the particle in joule

E is the total energy of the particle in joule

From the Lorentz force, for a particle with the parameters defined above, on an equilibrium orbit, in a magnetic field B:

$$\frac{\gamma m v^2}{R} = qvB$$

$$\gamma m v = qBR$$

$$E = E_0 + T$$

$$= mc^2 + T = \gamma mc^2$$

$$= \frac{mc^2}{\sqrt{1 - v^2/c^2}} = \frac{mc^2}{\sqrt{1 - \beta^2}}$$

$$\frac{E}{E_0} = \frac{E_0 + T}{E_0}$$

$$= \frac{\gamma mc^2}{mc^2}$$

$$= \gamma$$

$$= \frac{1}{\sqrt{1 - \beta^2}}$$

$$\beta = \frac{1}{\gamma} \sqrt{\gamma^2 - 1}$$

$$\gamma mv = \frac{\gamma mv}{mc} \quad mc$$

$$\gamma mv = mc \ \gamma\beta = qBR$$

$$= mc \ \gamma \ \frac{1}{\gamma} \ \sqrt{\gamma^2 - 1} = qBR$$

$$= mc \sqrt{\gamma^2 - 1} = qBR$$

$$mc^2\ (\gamma^2\text{-}1)\ =\ q^2B^2R^2$$

$$m^2c^2\ \left[(\frac{T+E_0}{E_0})^2 - 1\right] = q^2B^2R^2$$

$$mE_0\left[\frac{(T+E_0)^2 - E_0^2}{E_0^2}\right] = q^2B^2R^2$$

$$(T + E_0)^2 - E_0^2 = \frac{q^2B^2R^2E_0}{m} = p^2c^2$$

$$T^2 + 2TE_0 + E_o^2 - E_o^2 = \frac{q^2B^2R^2E_0}{m}$$

$$T^2 + 2TE_0 - \frac{q^2B^2R^2E_0}{m} = 0$$

$$T = -E_0 + \sqrt{E_0^2 + \frac{q^2B^2R^2E_0}{m}}$$

For low energies:

$$T = -E_0 + E_0\ \sqrt{1+\frac{q^2B^2R^2}{mE_0}}$$

$$T = -E_0 + E_0\ (1+\ \frac{q^2B^2R^2}{2mE_0})$$

$$= \frac{q^2B^2R^2}{2m}$$

In the equations above all the parameters are in M.K.S. units. Below the energy T is in MeV, the charge Q in terms of proton charge and the mass A in terms of proton mass:

$$T = \tfrac{1}{2}\,\frac{(1.6021917\mathrm{x}10^{-19})^2 Q^2}{1.67261\mathrm{x}10^{-27} A} \qquad B^2R^2$$

$$T = T(\mathrm{MeV})\ 1.6021917 \times 10^{-13}$$

$$T\,(\mathrm{MeV}) = \tfrac{1}{2}\,\frac{(1.6021917\mathrm{x}10^{-19})^2 B^2R^2}{1.6021917\mathrm{x}10^{-13}\mathrm{x}1.67261\mathrm{x}10^{-27}} \quad \frac{Q^2}{A}$$

$$= 47.89\, B^2R^2 \,\frac{Q^2}{A}$$

For A in terms of the atomic mass unit:

$$T\,(\mathrm{MeV}) = \tfrac{1}{2}\,\frac{(1.6021917\mathrm{x}10^{-19})^2 B^2R^2}{1.6021917\mathrm{x}10^{-13}\mathrm{x}1.6605\mathrm{x}10^{-27}} \quad \frac{Q^2}{A}$$

$$= 48.24\, B^2R^2 \,\frac{Q^2}{A}$$

$$= K\, \frac{Q^2}{A}$$

with $K = 48.24B^2R^2$.

REFERENCES

[Bec92] *Becker R., Review of Scientific instruments, Vol. 63 (1992) pp 2756-2758.*

[Bot] *Botha A. H., Personal communication.*

[Bro04] *Brown I. G., The physics and technology of ion sources Second Edition, Plasma physics 2004 pp 11, 17, 180, 182, 195, 196,200.*

[Bro89a] *Brown I. G., The Physics and Technology of Ion Sources, John Wiley & Sons, New York, 1989 pp 9-19.*

[Bro89b] *Brown I .G., The Physics and Technology of Ion Sources, John Wiley & Sons, New York, 1989 pp 23.*

[Bro89c] *Brown I .G., The Physics and Technology of Ion Sources, John Wiley & Sons, New York, 1989 pp 169-182.*

[Bro89d] *Brown I .G., The Physics and Technology of Ion Sources, John Wiley & Sons, New York, 1989 pp 281.*

[Bro89e] *Brown I .G., The Physics and Technology of Ion Sources, John Wiley & Sons, New York, 1989 pp 229.*

[Con00] *Conrads H., and Schmidt M., Plasma source Sci. Technol. Vol 9 (2000) 441-454*

[Con92] *Conradie J. L., Improved Proton Beam Quality and Intensity from a 200 MeV Cyclotron System Ph.D.-Thesis, unpublished (1992).*

[Eis05] *Eisa M. E., Optimization of Accelerator Optics and the Application of Nuclear Microscopy to the Biomedical Field, Ph.D Thesis, unpublished.*

[Gel69] *Geller R. et al, Proc. 1st Int. Conf. Ion Sources, Saclay 1969, 537.*

[Hil] *Hill C.E., Ion and Electron Ion Sources, CERN, Geneva, Switzerland.*

[Kel90] *Keller R., Nucl. Instr. and Meth. A 298 (1990) pp 247.*

[Mai02] *Maine P. M., Design and Optimisation of new Beam Lines for iThemba Laboratory for Accelerator Based Sciences (iThemba LABS), M.Sc. (Applied Radiation Science and Technology) Thesis, unpublished (2002), pp 4-12.*

[Max31] *Maxwell L.R., Rev. Sci. Instr. (1931) pp 2 and 129.*

[Mok02] *Mokoduwe P.S., Development of a Duoplasmatron Ion Source at iThemba LABS M.Sc. Thesis, unpublished (2002).*

[Nac76] *Technical Report of the Accelerator Task Group at iThemba LABS (1976) pp 7 and 8.*

[Nac89] *NAC Annual Report of 1989 page 3.*

[Nac90] *NAC Accelerator Annual Report of 1990 pp 3 and 4.*

[Sun98] Sun B. H., *Paper Presented at Cyclotron and their Applications 98, Caen, 14-19 June 1998 pp 423-426.*

[Tay93] Taylor T., and Mouris J. F., *Nucl. Instr. and Meth. in Phys. Res., A 336 (1993) pp 1-5.*

[Tra63] *Johnson W.C., McGraw-Hill Transmission Lines and Networks, (1963) page 105.*

[Wol95a] *Wolf B.H., Hand Book of Ion Source, John Willey and press, Inc, Oak Ridge (1995) pp 93-99.*

[Wol95b] *Wolf B.H., Hand Book of Ion Source, John Willey and press, Inc, Oak Ridge (1995) pp 109-118.*

[Wol95c] *Wolf B.H., Hand Book of Ion Source, John Willey and press, Inc, Oak Ridge (1995) pp 47.*

[Wol95d] *Wolf B.H., Hand Book of Ion Source, John Willey and press, Inc, Oak Ridge (1995) pp 121-128.*